THE JOURNAL OF BIOLOGICAL CHEMISTRY VOL. 289, NO. 17, pp. 12126–12144, April 25, 2014
© 2014 by The American Society for Biochemistry and Molecular Biology, Inc. Published in the U.S.A.

Histone Deacetylase-3 Mediates Positive Feedback Relationship between Anaphylaxis and Tumor Metastasis*

Received for publication, September 23, 2013, and in revised form, March 10, 2014 Published, JBC Papers in Press, March 11, 2014, DOI 10.1074/jbc.M113.521245

Sangkyung Eom[‡1], **Youngmi Kim**[‡1], **Deokbum Park**[‡], **Hansoo Lee**[§], **Yun Sil Lee**[¶], **Jongseon Choe**[‖], **Young Myeong Kim**[‖], **and Dooil Jeoung**[‡2]

From the Departments of [‡]*Biochemistry and* [§]*Biological Sciences, College of Natural Sciences,* [‖]*Graduate School of Medicine, Kangwon National University, Chunchon 200-701 and the* [¶]*College of Pharmacy, Ewha Womans University, Seoul 120-750, Korea*

Background: The relationship between anaphylaxis and tumor metastasis remains unknown at the molecular level.
Results: The miR-384/HDAC3 axis regulates an interaction between tumor cells and mast cells.
Conclusion: HDAC3 mediates a positive feedback loop between anaphylaxis and tumor metastasis.
Significance: HDAC3 can be a target for the development of allergy and cancer therapeutics.

Allergic inflammation has been known to enhance the metastatic potential of tumor cells. The role of histone deacetylase-3 (HDAC3) in allergic skin inflammation was reported. We investigated HDAC3 involvement in the allergic inflammation-promotion of metastatic potential of tumor cells. Passive systemic anaphylaxis (PSA) induced HDAC3 expression and FcεRI signaling in BALB/c mice. PSA enhanced the tumorigenic and metastatic potential of mouse melanoma cells in HDAC3- and monocyte chemoattractant protein 1-(MCP1)-dependent manner. The PSA-mediated enhancement of metastatic potential involved the induction of HDAC3, MCP1, and CD11b (a macrophage marker) expression in the lung tumor tissues. We examined an interaction between anaphylaxis and tumor growth and metastasis at the molecular level. Conditioned medium from antigen-stimulated bone marrow-derived mouse mast cell cultures induced the expression of HDAC3, MCP1, and CCR2, a receptor for MCP1, in B16F1 mouse melanoma cells and enhanced migration and invasion potential of B16F1 cells. The conditioned medium from B16F10 cultures induced the activation of FcεRI signaling in lung mast cells in an HDAC3-dependent manner. FcεRI signaling was observed in lung tumors derived from B16F10 cells. Target scan analysis predicted HDAC3 to be as a target of miR-384, and miR-384 and HDAC3 were found to form a feedback regulatory loop. miR-384, which is decreased by PSA, negatively regulated HDAC3 expression, allergic inflammation, and the positive feedback regulatory loop between anaphylaxis and tumor metastasis. We show the miR-384/HDAC3 feedback loop to be a novel regulator of the positive feedback relationship between anaphylaxis and tumor metastasis.

Allergen-induced pulmonary inflammation promotes metastasis of B16F1 melanoma cells to the lung in a CD4- and G-protein-coupled receptor-dependent manner (1). Mast cell-derived angiopoietin-1 plays a critical role in the growth of plasma cell tumors (2). Plasma cell tumors are closely related to mast cell infiltration and neovascularization (2), supporting a causal relationship between inflammation and tumor growth (2). Mast cells promote the growth of Hodgkin lymphomas by inducing neovascularization and fibrosis (3). Tumor cells are surrounded by infiltrating inflammatory cells, such as macrophages and mast cells, and tumor progression is closely related to the expression of mast cell chymase (mMCP-5), tryptases (mMCP-6 and -7), and carboxypeptidase A (mMC-CPA) (4).

Mast cells play a tumor-promoting role in many cancers (5) and are required for macroscopic expansion of Myc-induced pancreatic islet tumors (6). Mast cell-derived hypoxia-inducible factor-1α is necessary for promoting melanoma growth (7). Mast cells in the tumor microenvironment are involved in the development of tumor lymphatic vessels in some molecular subtypes of breast cancer (8). Mast cells migrate to the tumor site and are necessary for the growth of pancreatic ductal adenocarcinoma (9). Mast cell mediators, such as histamine and cannabinoids, promote invasion of cervical carcinoma cells (10). Inflammatory mast cells promote angiogenesis during squamous epithelial carcinogenesis via the mast cell-specific proteases MCP-4 and MCP-6 (11). Mast cells are activated by stem cell factor and released by tumor cells, and these activated mast cells exacerbate tumor immunosuppression by increasing T regulatory cell numbers, resulting in augmentation of the suppression of T cells (12). These reports suggest a causal relationship between allergic inflammation and tumor development.

Systemic anaphylaxis is an immediate hyper-acute reaction that is mediated by bioactive mediators, mostly from mast cells (13, 14). These mediators cause severe hypotension, decrease in body temperature, and increased β-hexosaminidase activity (13). Anaphylaxis requires activation of mast cells and basophils (15). Passive systemic anaphylaxis (PSA)[3] is achieved by cross-linking of FcεRI-bound allergen-specific IgE (16). Lyn but

* This work was supported by National Research Foundation Grants 2010-0021357, 2011-0010867, 2012H1B8A2025495, and C1008749-01-01 and by National R&D Program for Cancer Control, Ministry for Health and Welfare, Republic of Korea, Grant 1320160.
[1] Both authors contributed equally to this work.
[2] To whom correspondence should be addressed. Tel.: 82-33-250-8518; Fax: 82-33-242-0459; E-mail: jeoungd@kangwon.ac.kr.

[3] The abbreviations used are: PSA, passive systemic anaphylaxis; BMMC, bone marrow-derived mouse mast cell; DNP-HSA, dinitrophenyl-human serum albumin; PGES, prostaglandin E synthase; PGDH, prostaglandin dehydrogenase; EMT, epithelial mesenchymal transition; miRNA, microRNA.

Downloaded from http://www.jbc.org/ at Università degli Studi di Roma on June 18, 2017

not Fyn kinase controls IgG-mediated systemic anaphylaxis (16). Given the fact that mast cells promote tumor growth, it is probable that PSA promotes tumor growth and metastasis. Although allergic inflammation, such as allergen-induced pulmonary inflammation, is believed to enhance the metastatic potential of tumor cells, the effect of PSA on tumor metastasis and an interaction between anaphylaxis and tumor metastasis has not been explored yet.

Histone acetylation/deacetylation plays an important role in the regulation of inflammatory genes associated with allergic inflammation (17). The induction of cyclooxygenase (COX)-2, which occurs during allergic inflammation, is accompanied by degradation of histone deacetylase (HDAC) 1 (19). HDAC2 expression and activity are decreased in asthmatic subjects, smokers, and smoking asthmatic subjects (20). Trichostatin A, an inhibitor of HDACs, attenuates airway inflammation in animal models of asthma (21). HDAC3 is necessary for the induction of TNF-α, a cytokine increased during allergic inflammation, in cardiomyocytes during lipopolysaccharide stimulation (22). HDAC3, induced by antigen stimulation, interacts with FcϵRI and is necessary for allergic inflammation both *in vitro* and *in vivo* (23). Although we reported the role of HDAC3 in allergic skin inflammatory reactions, such as passive cutaneous anaphylaxis (23), the role of HDAC3 in PSA has not been investigated. Furthermore, the possible role of HDAC3 in mediating an interaction between tumor and mast cells remains.

MicroRNAs (miRNAs) are small, single-stranded noncoding RNAs that play important roles in the post-transcriptional regulation of gene expression in mammalian cells by regulating translation. The inhibition of mmu-miR-106a decreases interleukin (IL) 1–10 expression while increasing pro-inflammatory cytokine expression (24). Alveolar macrophage-derived vascular endothelial growth factor (VEGF) is necessary for allergic airway inflammation in asthmatic mice, and miR-20b negatively regulates the expression of VEGF (25). miR-1248 interacts with the IL-5 transcript in the 3′-untranslated region and serves as a positive regulator of IL-5 expression (26). Let-7 miRNA inhibits allergic lung airway inflammation by decreasing the expression of IL-5 (27). miRNA let-7a regulates the expression of IL-13, a cytokine necessary for allergic lung disease (28). The down-regulation of miR-145 inhibits Th2 cytokine production and airway hyper-responsiveness (29). These reports address the roles of miRNAs in allergic inflammation and in mediating the interaction between tumor and mast cells. To date, miRNAs that bind to and regulate the expression of HDAC3 and participate in mediating tumor and mast cell interaction have not been identified.

In this study, we examined the relationship between PSA and tumor metastasis, with the aim of delineating the PSA-mediated molecular mechanisms in enhancing the tumorigenic and metastatic potential of tumor cells. We investigated the effect of HDAC3 and the effect of MCP1, a target of HDAC3-mediated up-regulation, on PSA and the positive feedback relationship between anaphylaxis and tumor. We identified miR-384 as a novel regulator of HDAC3. We investigated the effect of miR-384 on allergic inflammation and on the tumor-mast cell interaction using a mouse melanoma model. In this study, we provide evidence that a miR-384/HDAC3 feedback regulatory loop acts as a novel regulator of the positive feedback relationship between anaphylaxis and tumor metastasis.

EXPERIMENTAL PROCEDURES

Cell Culture—Rat basophilic leukemia (RBL2H3) cells were obtained from the Korea Cell Line Bank (Seoul, Korea). Cells were grown in Dulbecco's modified Eagle's medium containing heat-inactivated fetal bovine serum, 2 mM L-glutamine, 100 units/ml penicillin, and 100 μg/ml streptomycin (Invitrogen). Cultures were maintained in 5% CO_2 at 37 °C. Bone marrow-derived mast cells (BMMC) and lung mast cells were isolated and maintained according to the standard procedures (30). Cancer cell lines used in this study were cultured in Dulbecco's modified minimal essential medium (DMEM; Invitrogen) supplemented with heat-inactivated 10% fetal bovine serum (FBS, Invitrogen) and antibiotics at 37 °C in a humidified incubator with a mixture of 95% air and 5% CO_2.

Chemicals and Reagents—Oligonucleotides used in this study were commercially synthesized by the Bionex Co. (Seoul, Korea). DNP-HSA and DNP-specific IgE antibody were purchased from Sigma. Chemicals used in this study were purchased from Sigma. All other antibodies were purchased from Cell Signaling Co. (Beverly, MA). Anti-mouse and anti-rabbit IgG-horseradish peroxidase-conjugated antibody was purchased from Pierce. Lipofectamine and Plus™ reagent for transfection were purchased from Invitrogen. Cytokine ELISA kit was purchased from Koma Biotech (Seoul, Korea).

Mice—Female 5–6-week-old BALB/c mice were purchased from Orient Co. (Seongnam, Korea). All animal care, experiments, and euthanasia were performed in accordance with protocols approved by the Kangwon National University Animal Research Committee (Chunchon, Korea). To measure tumorigenic potential, mouse melanoma B16F1 cells (1×10^6 cells in 100 μl of PBS), after induction of passive systemic anaphylaxis, were injected subcutaneously into the right flank of each mouse ($n = 5$). Tumor growth was evaluated by measuring the tumor diameters with calipers and calculating the tumor volumes using an approximated formula for a prolate ellipsoid as follows: volume $= ((a \cdot b^2)/2)$, where a is the longest axis of the tumor, and b is the shortest axis. After 3 weeks, the mice were sacrificed, and the final tumor volumes were measured. For lung metastasis experiments, B16F1 cells (1×10^6 cells in 0.2 ml of PBS), after induction of passive systemic anaphylaxis were injected into the tail vein of BALB/c mice. Fifteen days after IgE sensitization, the mice were sacrificed, and the tumor nodules on the surface of the lungs were counted under a dissecting microscope. H&E staining served to validate the identity of malignant colonies in the lungs of mice that had received tumor cells intravenously. For H&E staining, lung tumor tissue samples were fixed in 10% (v/v) buffered formalin, embedded in paraffin, sectioned at 4 μm, and then stained with hematoxylin and eosin.

Monitoring of Rectal Temperature—Changes in core body temperature associated with systemic anaphylaxis were monitored by measuring changes in rectal temperatures using a rectal probe coupled to a digital thermometer as described (31).

Downloaded from http://www.jbc.org/ at Università degli Studi di Roma on June 18, 2017

β-Hexosaminidase Activity Assays—The β-hexosaminidase activity assay was performed according to standard procedures (23).

Histamine Release Assay—Serum histamine level was measured according to the manufacturer's instructions (SPI-Bio). For serum histamine levels, blood from each mouse was collected by cardiac puncture under anesthesia.

Histological Analyses—Harvested tissues (lung) were frozen in optimal cutting temperature compound by Tissue Tek (OCT; Allegiance, McGaw, IL). Frozen tissues were cryosectioned (6–10 μm) and placed on positively charged glass slides. Nonspecific binding of antibodies was blocked by incubation with 1% bovine serum albumin (BSA) for 1 h before incubation with primary antibodies. The following primary antibodies were used for single and double staining: anti-Fcε$R1_\beta$ (1:100) and anti-HDAC3 (1:100, Santa Cruz Biotechnology); anti-MCP1 (1:50, Abcam, UK), and FITC-conjugated anti-CD11b antibody (1:100, Pierce). The sections were incubated with primary antibodies overnight at 4 °C. After washing, secondary antibodies were applied at 1:100 or 1:200 dilutions for 1 h. We used goat anti-rabbit IgG-FITC (Santa Cruz Biotechnology) for HDAC3, rabbit anti-goat Alexa 546 for MCP1 and Fcε$R1_\beta$ staining (Molecular Probes). DAPI (Molecular Probes) was added to stain nuclei. Confocal images were acquired using a confocal laser scanning microscope (FV-1000, Olympus). Immunohistochemical staining of lung tissues was also performed using an established avidin-biotin detection method (Vectastain ABC kit, Vector Laboratories Inc., Burlingame, CA). Briefly, 4–6-μm-thick sections of the paraffin-embedded tissue blocks were cut, mounted on positively charged glass slides, and dried in an oven at 56 °C for 30 min. The sections were deparaffinized in xylene and then rehydrated in graded ethanol and water. Endogenous peroxidase was blocked by incubation in 3% (v/v) hydrogen peroxide for 15 min. Antigen retrieval was accomplished by pretreatment of the sections with citrate buffer at pH 6.0 for 20 min at 56 °C in a microwave oven and then allowing the sections to cool for 30 min at room temperature. Nonspecific endogenous protein binding was blocked using 1% bovine serum albumin (BSA). The sections were then incubated with primary antibodies overnight at 4 °C. The following primary antibodies were used for single and double staining: anti-c-kit (1:100, Santa Cruz Biotechnology), anti-HDAC3 (1:100, Santa Cruz Biotechnology), and anti-MCP1 (1:50, Abcam). After washing, biotinylated secondary antibodies were applied at 1:100 or 1:200 dilutions for 1 h. Color was developed with diaminobenzidine (Vector Laboratories, Inc.). Sections were counterstained with Mayer's hematoxylin. Sections incubated without primary antibody served as controls. To visualize tissue mast cells, the sections were stained with 0.1% olivine blue (Sigma) in 0.1 N HCl for 15 min.

Immunofluorescence Staining—RBL2H3 cells were seeded onto glass coverslips in 24-well plates and were sensitized with DNP-specific IgE (100 ng/ml) for 16 h. After stimulation with DNP-HSA (100 ng/ml) for 1 h, cells were fixed with 4% paraformaldehyde (v/v) for 10 min and then permeabilized with 0.4% Triton X-100 for 10 min. Nonspecific antibody-binding sites were blocked by incubation with 1% BSA in TBST for 30 min. Cells were then incubated with primary antibody specific to HDAC3 (1:100; Santa Cruz Biotechnology) or FcεRI_β (1:100; Santa Cruz Biotechnology) for 2 h, followed by washing with TBS-T three times. Anti-goat IgG-FITC (for detection of HDAC3) or anti-rabbit Alexa Fluor 586 (for detection of FcεRI_β) secondary antibody (Molecular Probes) was added to cells and incubated for 1 h. Coverslips were then washed and mounted by applying Mount solution (Biomeda, Foster City, CA). Fluorescence images were acquired using a confocal laser scanning microscope and software (Fluoview version 2.0) with a × 60 objective (Olympus FV300, Tokyo, Japan). To examine the effect of miR-384 on the co-localization of HDAC3 with FcεRI, RBL2H3 cells were transfected with control mimic (10 nM) or miR-384 mimic (10 nM). The next day, cells were sensitized with DNP-specific IgE (100 ng/ml) for 24 h, followed by stimulation with DNP-HSA (100 ng/ml) for 1 h. Immunofluorescence staining was performed.

Transfection—Transfections were performed according to the manufacturer's instructions. Lipofectamine and Plus reagents (Invitrogen) were used. The construction of siRNA was carried out according to the instruction manual provided by the manufacturer (Ambion, Austin, TX). For miR-384 knockdown, cells were transfected with 10 nM oligonucleotide (inhibitor) with Lipofectamine 2000 (Invitrogen), according to the manufacturer's protocol. The sequences used were 5′-ACAUUGCCUAGGAAUUGUUUACA-3′ (miR-384 inhibitor) and 5′-UUCUCCGAACGUGUCACGUTT-3′ (control inhibitor).

Western Blot Analysis—Western blot and immunoprecipitation were performed according to the standard procedures (23). For analysis of proteins from tissues, frozen samples were grounded to a fine powder using a mortar and pestle over liquid nitrogen. Proteins were solubilized in RIPA buffer containing protease inhibitors, and insoluble material was removed by centrifugation.

Cytokine Arrays—Expression levels of cytokine/chemokines were determined by using a ProteomProfiler™ human angiogenesis antibody array kit (R&D Systems, Minneapolis, MN) according to the manufacturer's instructions.

RNA Extraction and Quantitative Real Time PCR—Total miRNA was isolated using the *mir*VanamiRNA isolation kit (Ambion). miRNA was extended by a poly(A) tailing reaction using the A-Plus poly(A) polymerase tailing kit (Cell Script). cDNA was synthesized from miRNA with poly(A) tail using a poly(T) adaptor primer and qScript™ reverse transcriptase (Quanta Biogenesis). Expression levels of miR-384b was quantified with SYBR Green quantitative RT-PCR kit (Ambion) using an miRNA-specific forward primer and a universal poly(T) adaptor reverse primer. The expression of miR-384 was defined based on the threshold (C_t), and relative expression levels were calculated as $2^{-(C_t \text{ of miR-384}) - (C_t \text{ of U6})}$ after normalization with reference to expression of U6 small nuclear RNA. For quantitative PCR, SYBR PCR Master Mix (Applied Biosystems) was used in a CFX96 Real Time System thermocycler (Bio-Rad).

Chromatin Immunoprecipitation (ChIP) Assay—Assays were performed according to the manufacturer's instruction (Upstate). The HDAC3 antibody immunoprecipitates were reverse cross-linked. PCR was done on the phenol/chloroform-

Downloaded from http://www.jbc.org/ at Università degli Studi di Roma on June 18, 2017

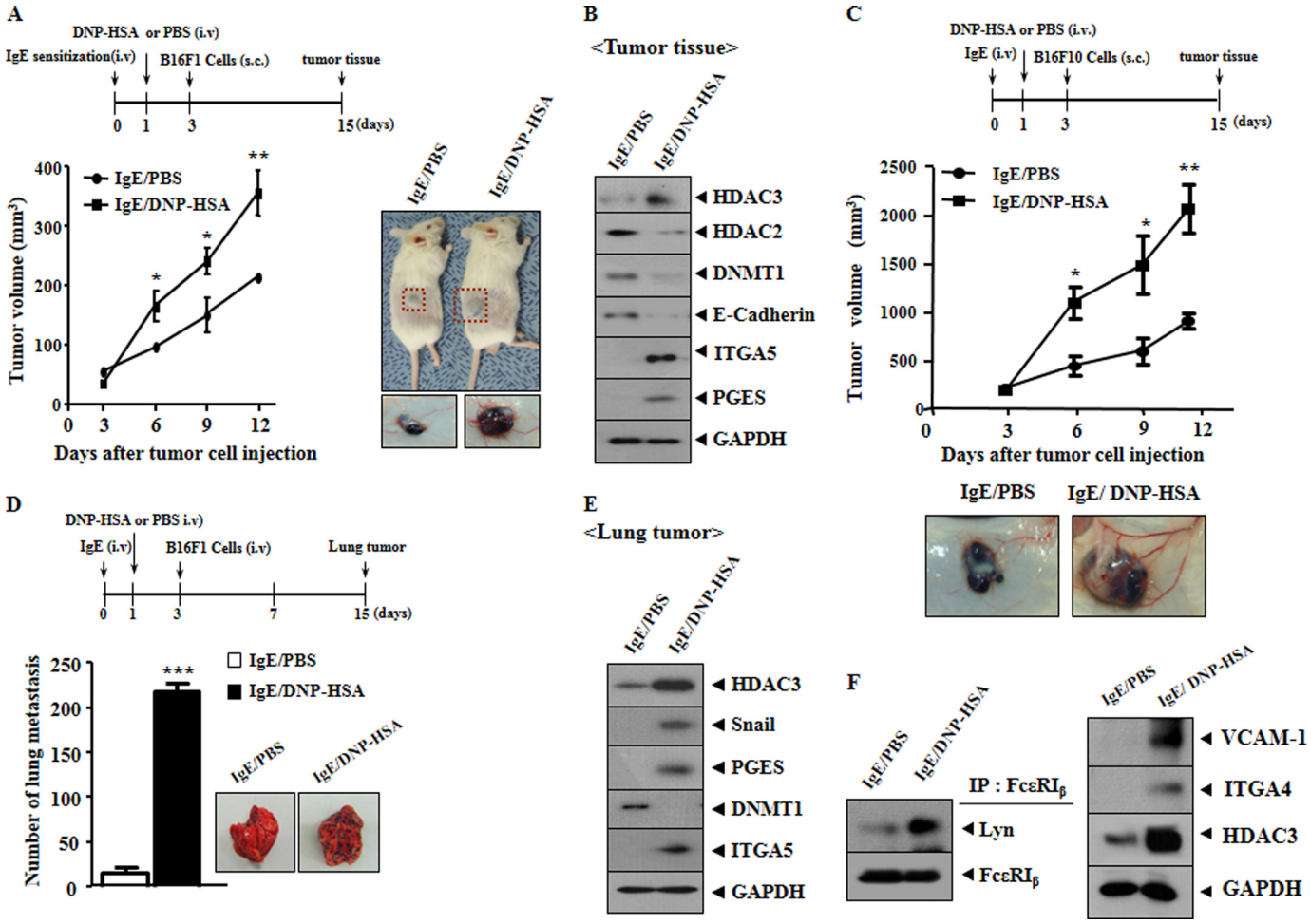

FIGURE 1. **PSA enhances the tumorigenic and metastatic potential of mouse melanoma cells.** *A*, BALB/c mice were sensitized to DNP-specific IgE (0.5 μg/kg) by i.v. injection. The next day, BALB/c mice were given an i.v. injection of DNP-HSA (250 μg/kg). Each flank of the mouse received injection of B16F1 melanoma cells (2×10^5) on day 3 of the time line. On the day 15 of the time line, the tumor volumes were measured. Each experimental group consisted of five mice. Representative images from five animals of each experimental group are shown. The mean ± S.E. of three independent experiments is shown. *, $p < 0.05$; **, $p < 0.005$. *B*, 15 days after injection of DNP-specific IgE, lysates were isolated from tumor tissue and subjected to Western blot analysis. *C*, protocol was the same as in *A* except that B16F10 cells were injected. *D*, BALB/c mice were sensitized to DNP-specific IgE (0.5 μg/kg) by an i.v. injection. The next day, BALB/c mice were given an i.v. injection of DNP-HSA (250 μg/kg). B16F1 melanoma cells (2×10^5) were injected into the tail vein of BALB/c mouse on the day 3 of the time line. Fifteen days after injection of IgE, lung tissues were isolated and the number of tumor nodules was counted to measure the extent of lung metastasis. Representative images from five animals of each experimental group are shown. The mean ± S.E. of three independent experiments is shown. ***, $p < 0.0005$. *E*, 15 days after injection of DNP-specific IgE, lysates were isolated from lung tumor tissue and subjected to Western blot analysis. *F*, lysates from B16F10 cell-derived tumor tissue were isolated and subjected to immunoprecipitation (*IP*) with anti-FcϵRI$_\beta$ (2 μg/ml), followed by Western blot analysis (*left panel*). Tissue lysates were also subjected to Western blot analysis (*right panel*).

extracted DNA with specific primers of the MCP1 promoter (5′-AAA TAG AGG GGT TGG GGG AG-3′ (sense) and 5′-CCG AGA CTC GAA CTG CAC AT-3′ (antisense)), and the sequences were used to examine the binding of HDAC3 to the MCP1 promoter sequences. To examine binding of HDAC3 to the miR-384 promoter sequences, specific primers of the *miR-384* promoter-1 sequences (5′-TGTCTCGCATCCAGC-CTAAG-3′ (sense) and 5′-TTCCGCTGCAAGAGAAATA-ACC-3′ (antisense)) and *miR-384* promoter-2 sequences (5′-TCAGCGAACCAGCTCACAAT-3′ (sense) and 5′-GTCT-TTCATTCTCCACCCAAGC-3′ (antisense)) were used.

Cellular Invasion Assays—The invasive potential of B16 F1 cells was determined by using a transwell chamber system with 8-μm pore polycarbonate filter inserts (Costar, Acton, MA). The lower and upper sides of the filter were coated with gelatin and Matrigel, respectively. To obtain conditioned medium, the IgE-sensitized BMMCs were preincubated with nMCP1 antibody (10 μg/ml) or isotype-matched control IgG (10 μg/ml) for 12 h, followed by stimulation with DNP-HSA (100 ng/ml) or PBS for 4 h. The trypsinized B16F1 cells (2×10^4) in the conditioned medium containing 0.1% bovine serum albumin were then added to each upper chamber of the transwell. B16F1 cells were seeded in M199 containing 20% FBS in the lower chamber, and cells were incubated at 37 °C for 14 h. The cells were fixed with methanol, and the invaded cells were stained and counted.

IgE-dependent Passive Systemic Anaphylaxis—For induction of systemic anaphylaxis, BALB/c mice were sensitized by i.v. injection of DNP-specific IgE (0.5 μg/kg). The next day, sensitized mice were challenged by i.v. injection of DNP-HSA (250 μg/kg). The following day, trypsinized B16F1 or B16F10 mouse melanoma cells in suspension were inoculated into each flank of the mouse to examine the effect of systemic anaphylaxis on tumorigenic potential. To determine the effect of HDAC3 on

Downloaded from http://www.jbc.org/ at Università degli Studi di Roma on June 18, 2017

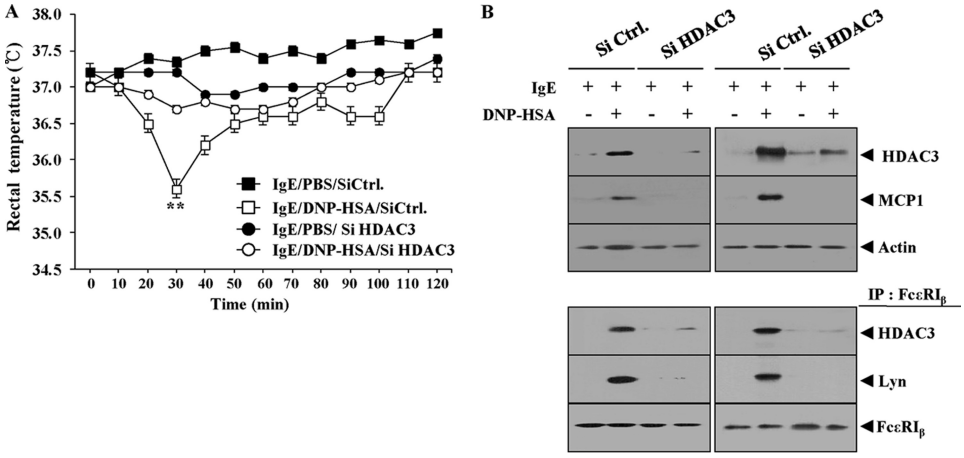

FIGURE 2. **HDAC3 is necessary for PSA.** *A,* BALB/c mice were injected with control (scrambled) siRNA (100 nM) or HDAC3 siRNA (100 nM) via the tail vein. The next day, BALB/c mice were injected with DNP-specific IgE (0.5 μg/kg) via the tail vein. The following day, BALB/c mice were injected i.v. with DNP-HSA (250 μg/kg), and rectal temperatures were measured. Each experimental group consisted of five mice. The means ± S.E. of three independent experiments are depicted. *SiCtrl* denotes scrambled siRNA. *B,* 2 h after injection of DNP-HSA, lung tissue lysates were isolated and subjected to Western blot analysis (*upper panel*). Lung tissue lysates were also immunoprecipitated (*IP*) with the indicated antibody (2 μg/ml), followed by Western blot analysis (*lower panel*).

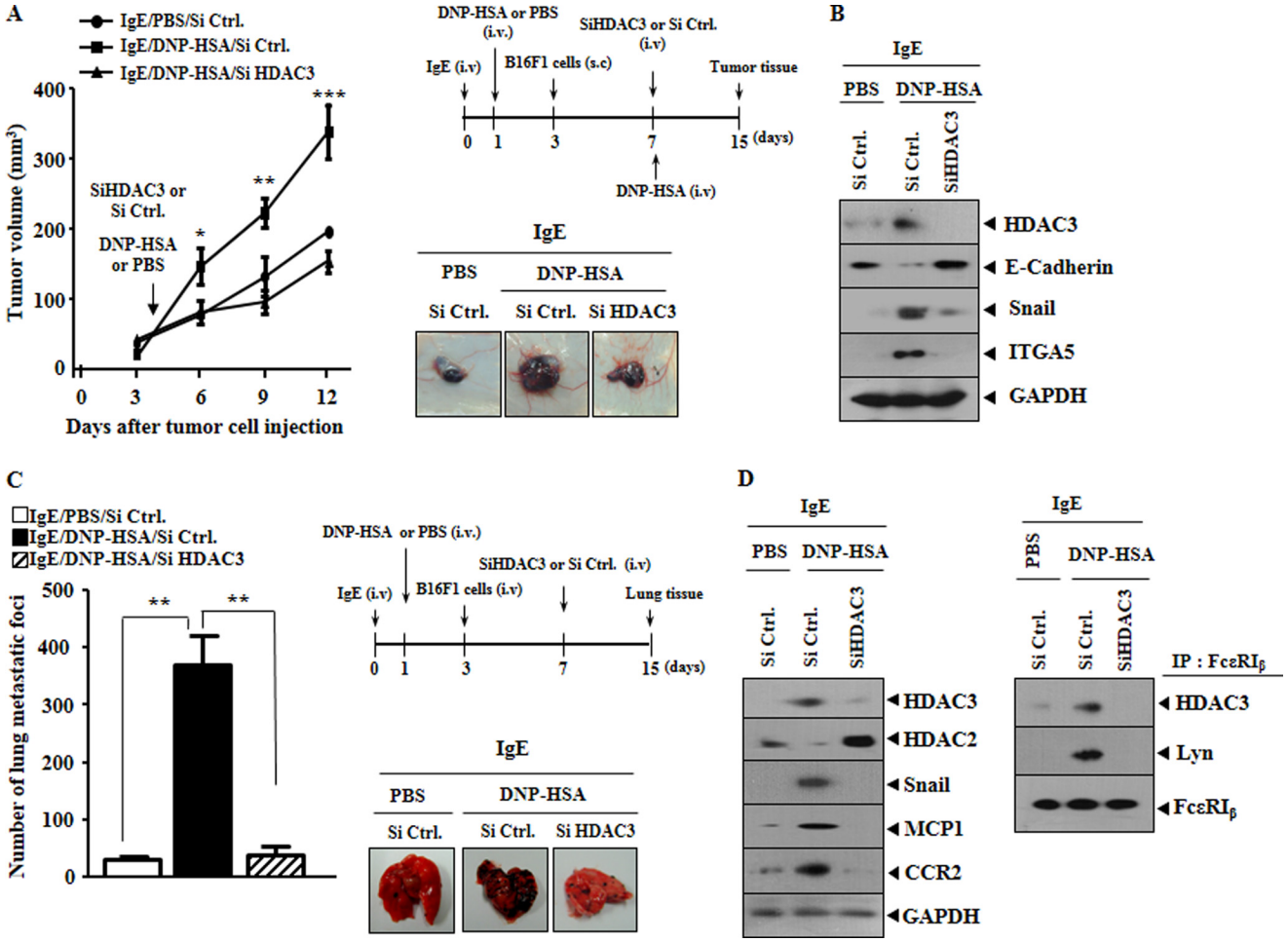

FIGURE 3. **HDAC3 is necessary for enhanced tumorigenic and metastatic potential of B16F1 melanoma cells by PSA.** *A,* BALB/c mice were sensitized to DNP-specific IgE (0.5 μg/kg) by an i.v. injection. The next day, BALB/c mice were given an i.v. injection of DNP-HSA (250 μg/kg). Each flank of the mouse received injection of B16F1 melanoma cells (2×10^5) on day 3 of the time line. Four days after injection of tumor cells, BALB/c mice were given an i.v. injection of scrambled siRNA (100 nM) or HDAC3 siRNA (100 nM) along with DNP-HSA (250 μg/kg) or PBS. On day 15 of the time line, the tumor volumes were measured. Each experimental group consisted of five mice. Representative images from five animals of each experimental group are shown. The mean ± S.E. of three independent experiments is depicted. *Ctrl,* control. *, $p < 0.05$; **, $p < 0.005$; ***, $p < 0.0005$. *B,* lysates isolated from tumor tissue of mice from each experimental group was subjected to Western blot analysis. *C,* BALB/c mice were given an i.v. injection with DNP-specific IgE(0.5 μg/kg). The next day, mice were treated with DNP-HSA (250 μg/kg) or PBS. On the day 3 of the time line, mice were given an i.v. injection with B16F1 cells. On day 7 of the time line, mice were given an i.v. injection of scrambled siRNA (100 nM) or HDAC3 siRNA (100 nM). The extent of lung metastasis was measured. Each group consisted of five mice. **, $p < 0.005$. *D,* lysates isolated from lung tumor tissue of mice from each experimental group were immunoprecipitated (*IP*) with the indicated antibody (2 μg/ml), followed by Western blot analysis (*right panel*). Tissue lysates were also subjected to Western blot analysis (*left panel*).

Downloaded from http://www.jbc.org/ at Università degli Studi di Roma on June 18, 2017

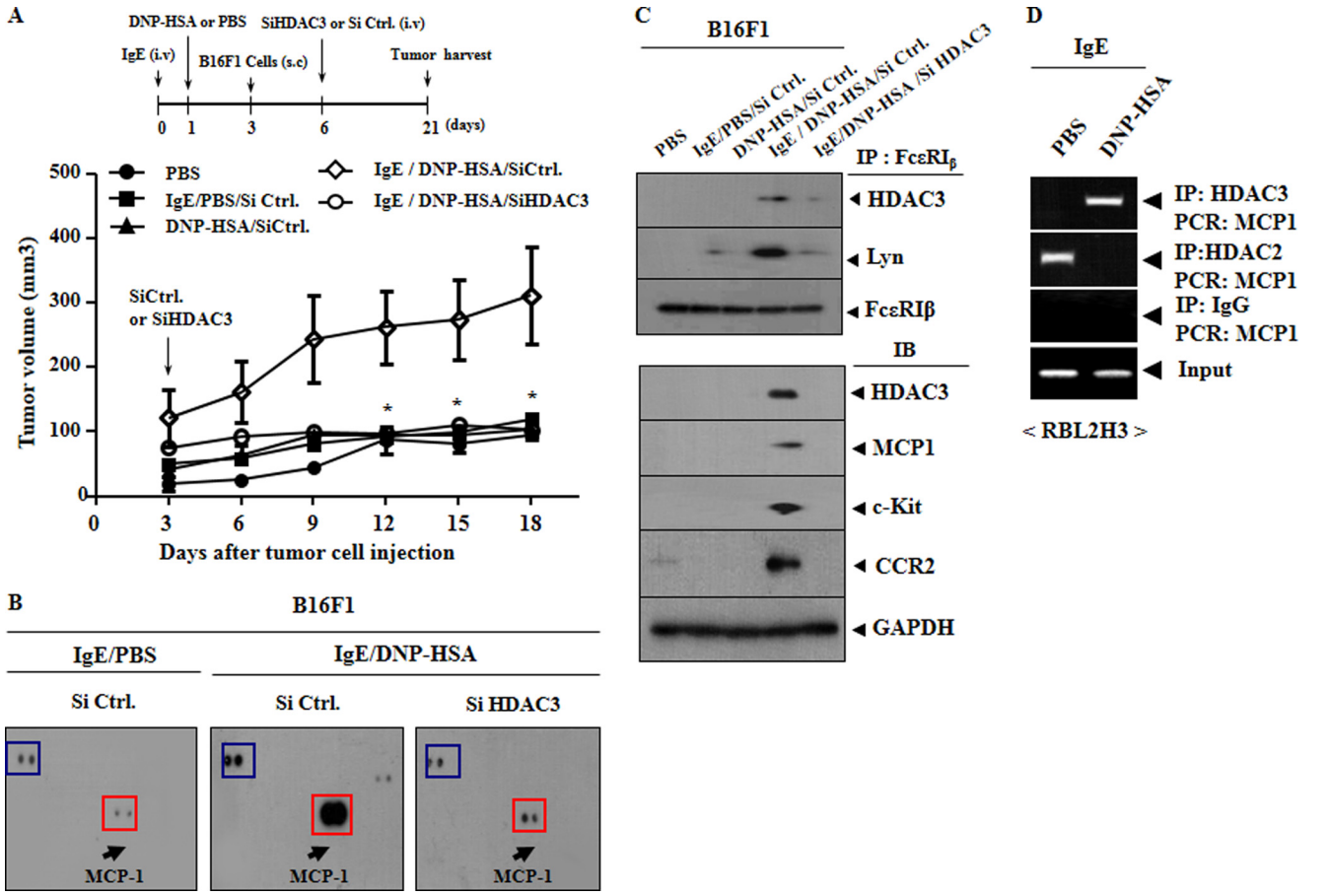

FIGURE 4. **HDAC3 regulates the expression of MCP1 and enhances tumorigenic potential of B16F1 melanoma cells.** *A,* BALB/c mice were given an i.v. injection of DNP-specific IgE (0.5 μg/kg). The next day, mice were given an i.v. injection of DNP-HSA (250 μg/kg). Each flank of the mouse received injections of B16F1 melanoma cells (2×10^5) on day 3 of the time line. On day 6 of the time line, BALB/c mice were given an i.v. injection of scrambled siRNA (100 nM) or HDAC3 siRNA (100 nM). Each group consisted of five mice. The mean ± S.E. of three independent experiments is depicted.*, $p < 0.05$. *B,* blood serum was collected from BALB/c mice of each experimental group. Eighteen days after injection of B16F1 cells, serum of BALB/c mice of each experimental group was incubated with a cytokine array. *C,* lysates prepared from lungs of BALB/c mice were immunoprecipitated (*IP*) with the indicated antibody (each at 2 μg/ml), followed by Western blot analysis (*upper panel*). The same tissue lysates were subjected to Western blot analysis (*lower panel*). *D,* ChIP assays were performed in antigen-stimulated RBL2H3 cells using the indicated antibody (2 μg/ml).

the tumorigenic potential of melanoma cells, control (scrambled) siRNA (100 nM) or HDAC3 siRNA (100 nM) was injected i.v. into the tail vein of BALB/c mice 3 days after tumor cell injection. To determine the effect of PSA on the metastatic potential of mouse melanoma cells, BALB/c mice were injected with 2,4-dinirophnyl (DNP)-specific IgE (0.5 μg/kg) via the tail vein. The next day, BALB/c mice were injected i.v. with DNP-HSA (250 μg/kg). Two days after injection of DNP-HSA, mouse melanoma B16F1 cells were injected, via tail vein, into BALB/c mice. To determine the effect of PSA on the tumorigenic potential of mouse melanoma cells, BALB/c mice were injected with DNP-specific IgE via the tail vein. The next day, BALB/c mice were injected i.v. with antigen DNP-HSA (250 μg/kg). Two days after injection of DNP-HSA, B16F1 mouse melanoma cells were injected into the flanks of each BLAB/c mouse.

Statistical Analysis—Data were analyzed and graphed using GraphPad Prism statistics program (GraphPad Prism software). Results are presented as means ± S.E. Statistical analysis was performed using *t* tests with differences between means considered significant when $p < 0.05$.

RESULTS

Passive Systemic Anaphylaxis Enhances Tumorigenic and Metastatic Potential of Mouse Melanoma B16F1 Cells—Allergen-induced pulmonary anaphylaxis promotes metastases of mouse melanoma cells (1). In this, CD4 and G-protein-coupled receptors are necessary for asthmatic condition-induced enhanced metastatic potential of melanoma cells. This suggests a functional role for mast cells in promoting the metastatic potential of mouse melanoma cells. In this study, we monitored the effect of PSA on the tumorigenic and metastatic potential of tumor cells. Induction of PSA enhanced the tumorigenic potential of B16F1 mouse melanoma cells (Fig. 1*A*). Western blotting of lung tumor tissue lysates showed that PSA increased the expression of allergic reaction markers, such as HDAC3, integrin α5, and prostaglandin E synthase (PGES) (Fig. 1*B*). HDAC3 interacts with Snail to repress transcription of various genes such as prostaglandin dehydrogenase (PGDH) (32). The down-regulation of PGDH is associated with the induction of PGES (32). HDAC3 interacts with Snail in antigen-stimulated RBL2H3 cells (data not shown), and HDAC3 may, in association with Snail, bind to the PGDH promoter sequences, result-

Downloaded from http://www.jbc.org/ at Università degli Studi di Roma on June 18, 2017

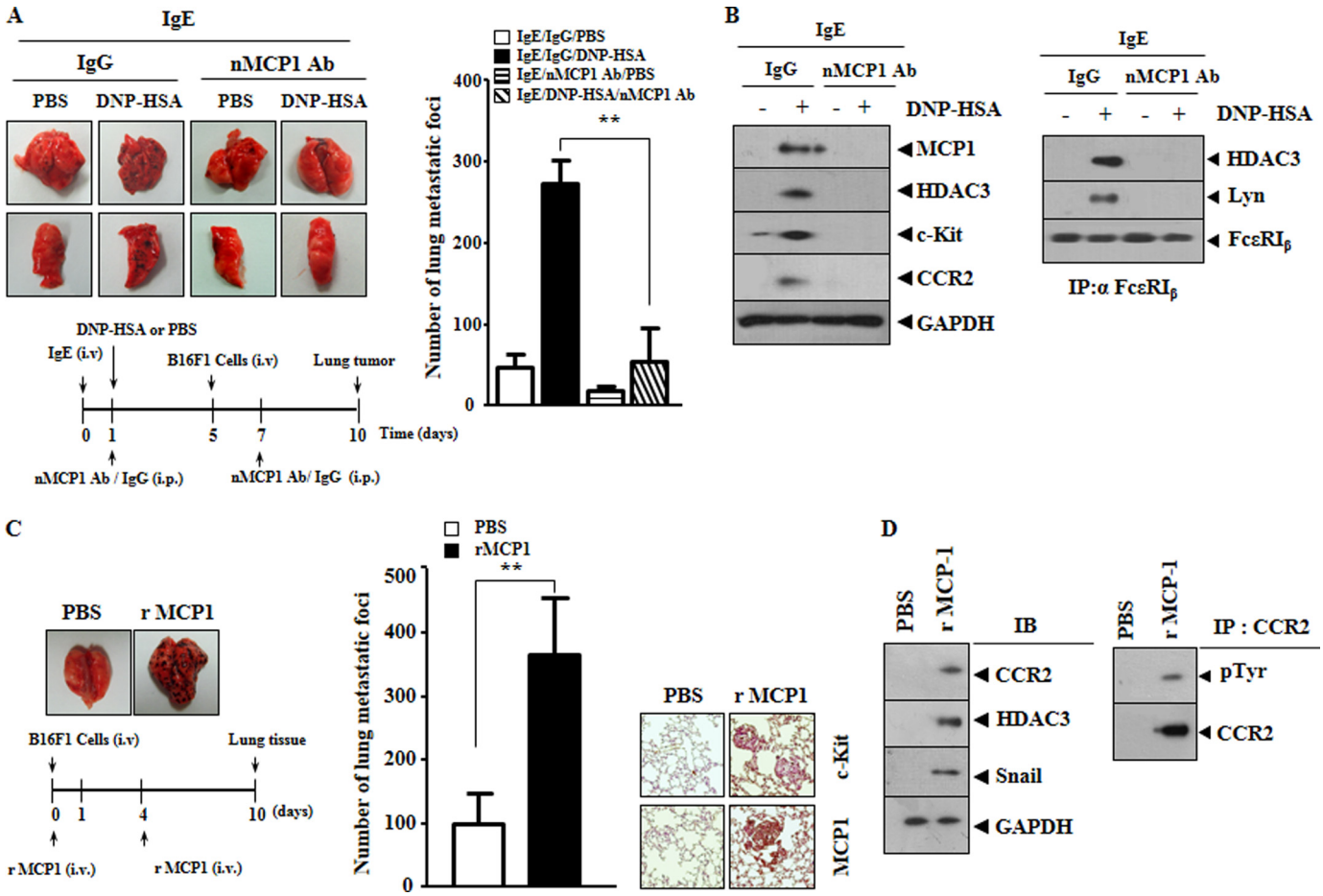

FIGURE 5. **MCP1 is necessary for enhanced metastatic potential of B16F1 melanoma cells by PSA.** *A*, on day 0 of the time line, BALB/c mice were given an i.v. injection of DNP-specific IgE (0.5 μg/kg). The next day, BALB/c mice were given an i.v. injection of DNP-HSA (250 μg/kg) along with an intraperitoneal injection of neutralizing MCP1 antibody (*nMCP1 Ab*, 10 μg/kg) or isotype-matched IgG (10 μg/kg). On the day 5 of the time line, BALB/c mice were given an i.v. injection of B16F1 cells. On day 7 of the time line, BALB/c mice were given an intraperitoneal injection of neutralizing MCP1 antibody (10 μg/kg) or isotype-matched IgG (10 μg/kg). On day 10 of the time line, the extent of lung metastasis was determined. *, $p < 0.05$. *B*, lung tumor tissue lysates were isolated from each mouse of each experimental group and immunoprecipitated (*IP*) with the indicated antibody (2 μg/ml), followed by Western blot analysis (*right panel*). Tumor lysates were also subjected to Western blot analysis (*left panel*). *C*, on day 0 of the time line, BALB/c mice were given an i.v. injection of B16F1 cells (2×10^5) along with an intraperitoneal injection of mouse recombinant MCP1 protein (10 μg/kg) or PBS. On day 4 of the time line, BALB/c mice were given an intraperitoneal injection of mouse recombinant MCP1 protein (10 μg/kg) or PBS. Ten days after injection of B16F1 cells, the extent of lung metastasis of B16F1 melanoma cells was determined. Immunohistochemical staining was also performed. **, $p < 0.005$. *D*, lung tumor tissue lysates were isolated from each mouse of each group of mice and were immunoprecipitated with the indicated antibody, followed by Western blot analysis (*right panel*). Tumor lysates were also subjected to Western blot analysis (*left panel*). *IB*, immunoblot.

ing in the decreased expression of PGDH and thereby the induction of PGES. PSA decreased the expression of HDAC2, DNA methyltransferase (DNMT) 1, and E-cadherin (Fig. 1*B*). We previously reported the decreased expression of HDAC2 in antigen-stimulated RBL2H3 cells (30). DNMT1 acts as a negative regulator of allergic skin inflammation (33). PSA also enhanced the tumorigenic potential of highly malignant B16F10 mouse melanoma cells (Fig. 1*C*).

We next examined the effect of PSA on the metastatic potential of mouse melanoma cells. BALB/c mice were injected with DNP-specific IgE via the tail vein and subsequently challenged with DNP-HSA (Fig. 1*D*). Two days after injection of DNP-HSA, B16F1 cells were injected into the BALB/c mouse. PSA enhanced metastasis of B16F1 cells to the lung (Fig. 1*D*), and it increased the expression of HDAC3, Snail, PGES, and integrin α5 (Fig. 1*E*). PSA induced the activation of FcϵRI signaling, as indicated by an interaction between FcϵRI$_\beta$ and Lyn (Fig. 1*F*). Western blotting analysis of lung tumor tissue lysates showed PSA induced increased expression of adhesion molecules such as integrin α4 and VCAM-1 (Fig. 1*F*). Taken together, these results suggest that the PSA-mediated enhancement of the tumorigenic and metastatic potential of mouse melanoma cells involve the activation of mast cells and FcϵRI signaling.

HDAC3 Is Necessary for PSA—The role of HDAC3 in allergic skin inflammation has been reported (23). Because the PSA-mediated enhancement of tumorigenic and metastatic potential involved the increased expression of HDAC3 (Fig. 1, *B* and *D*), we examined the effect of HDAC3 on PSA by assessing the effect of siRNA-mediated knockdown of HDAC3 on PSA. BALB/c mice were injected with scrambled siRNA or HDAC3 siRNA, followed by injection with DNP-specific IgE and challenge with DNP-HSA. The *in vivo* down-regulation of HDAC3 prevented the antigen from decreasing the rectal temperature of the mice (Fig. 2*A*). Western blotting analysis of lung tissue lysates revealed the induction of HDAC3 and MCP1 by PSA (Fig. 2*B*). The *in vivo* down-regulation of HDAC3 also pre-

Downloaded from http://www.jbc.org/ at Università degli Studi di Roma on June 18, 2017

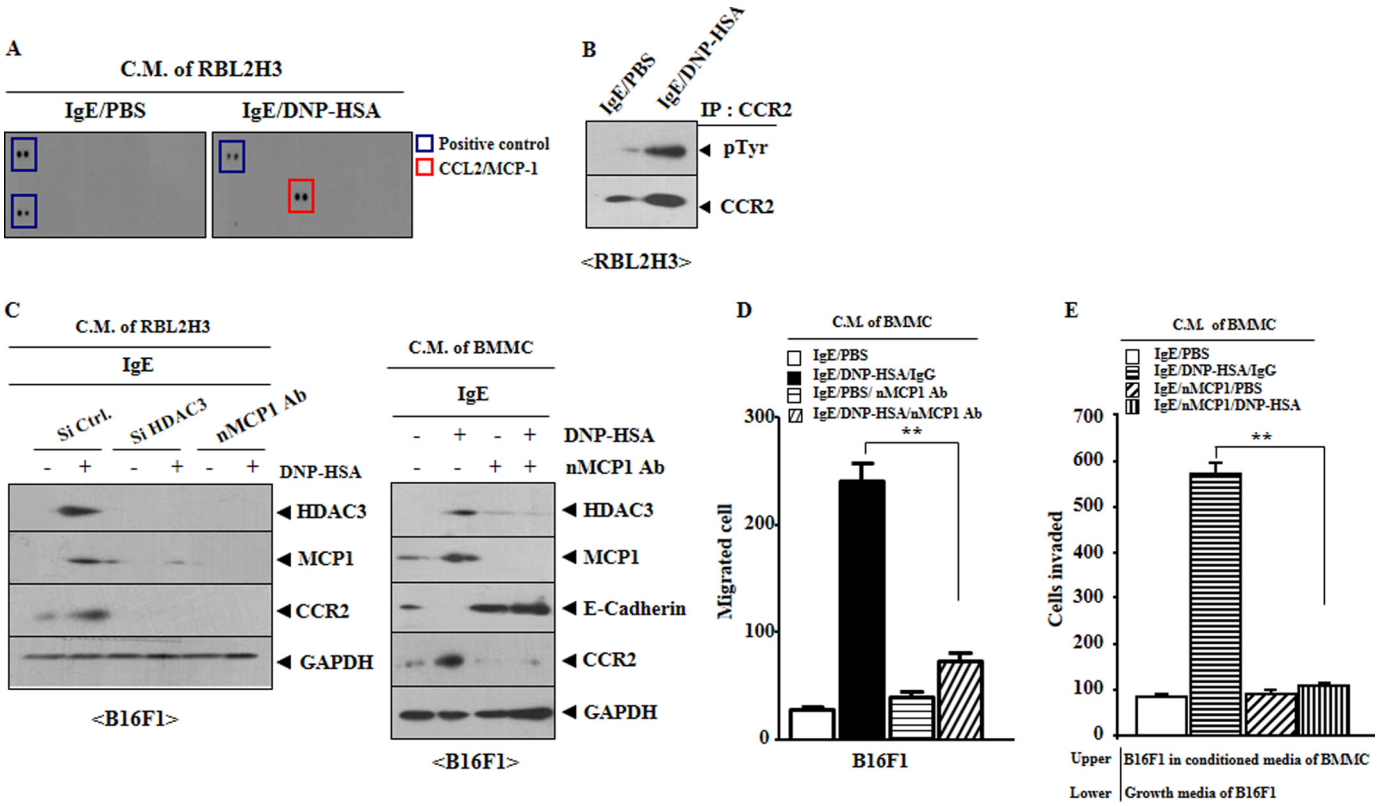

FIGURE 6. **MCP1 is necessary for enhanced invasion and migration potential of B16F1 cells.** *A*, IgE-sensitized RBL2H3 cells were stimulated with or without DNP-HSA (100 ng/ml) for 1 h. The conditioned medium (*C.M.*) of RBL2H3 cells of each experimental group was incubated with the cytokine array. *B*, same as *A* except that cell lysates were immunoprecipitated (*IP*) with the indicated antibody (2 μg/ml), followed by Western blot analysis. *C*, RBL2H3 cells were transiently transfected with Sicontrol (10 nM) or SiHDAC3 (10 nM). The next day, cells were sensitized with DNP-specific IgE (100 ng/ml), followed by stimulation with DNP-HSA (100 ng/ml) for 2 h. Conditioned medium was prepared and added to B16F1 cells in serum-free medium in a 1:1 ratio. The IgE-sensitized RBL2H3 or BMMCs were preincubated with nMCP1 antibody (10 μg/ml) or isotype-matched IgG (10 μg/ml) for 2 h, followed by stimulation with DNP-HSA (100 ng/ml) for 2 h. Then the medium from RBL2H3 or BMMC cultures was added to B16F1 cells in serum-free medium in 1:1 ratio. At 24 h after addition of each conditioned medium, Western blot analysis was performed. *D*, IgE-sensitized BMMCs were preincubated with or without nMCP1 antibody (10 μg/ml) for 2 h, followed by stimulation with DNP-HSA (100 ng/ml) for 2 h. This conditioned medium from BMMCs was added to B16F1 cells in serum-free medium in 1:1 ratio. Wounds were made immediately to the B16F1 cells, and wound migration assays were performed. Forty eight hours later, the number of migrated B16F1 cells was determined under light microscope. *, $p < 0.005$. *E*, using an 8-μm Matrigel-coated Boyden chamber, B16F1 melanoma cells (2×10^4) in conditioned medium of BMMCs treated as indicated were plated in the upper chamber, and the growth medium for B16F1 cells was placed in the lower chamber. Twenty four hours later, the number of invading cells per a ×200 field in response to either conditioned medium (*C.M.*) with or without nMCP1 was determined by H&E staining. **, $p < 0.005$.

vented the PSA-mediated FcϵRI$_\beta$-Lyn and FcϵRI$_\beta$ and HDAC3 interactions (Fig. 2*B*). Taken together, these results suggest that HDAC3 is necessary for PSA.

HDAC3 Is Necessary for Enhanced Tumorigenic and Metastatic Potential of Mouse Melanoma Cells by PSA—Because HDAC3 was necessary for PSA, we examined the role of HDAC3 in the enhanced tumorigenic and metastatic potential by PSA. For this, BALB/c mice were injected with DNP-specific IgE via the tail vein (Fig. 3*A*). The next day, BALB/c mice were injected i.v. with DNP-HSA (Fig. 3*A*). Two days after injection of DNP-HSA, B16F1 cells were injected into the flanks of each BLAB/c mouse (Fig. 3*A*). Four days after injection of B16 F1 cells, siHDAC3 or siControl was injected i.v. into BALB/c mouse (Fig. 3*A*). The *in vivo* down-regulation of HDAC3 suppressed PSA-mediated enhancement of tumorigenic potential (Fig. 3*A*). The *in vivo* down-regulation of HDAC3 decreased the expression of Snail and integrin α5 while increasing the expression of E-cadherin (Fig. 3*B*). These data suggest PSA-mediated tumorigenesis may involve the epithelial mesenchymal transition (EMT). The *in vivo* down-regulation of HDAC3 attenuated the metastatic potential of B16F1 cells by PSA (Fig. 3*C*), suggesting that PSA-mediated promotion of metastatic potential may occur in an HDAC3-dependent manner. The *in vivo* down-regulation of HDAC3 decreased the expression of Snail, MCP1, and CCR2, a receptor for MCP1, while increasing the expression of HDAC2, in lung tumor tissue (Fig. 3*D*). Immunoprecipitation analysis showed that PSA stimulated FcϵRI$_\beta$-HDAC3 and FcϵRI$_\beta$-Lyn interactions (Fig. 3*D*), although these effects were attenuated by the down-regulation of HDAC3 (Fig. 3*D*). Taken together, these results suggest that HDAC3 is necessary for enhanced tumorigenesis and metastasis of B16F1 cells and the activation of FcϵRI signaling by PSA.

MCP1 Is Regulated by HDAC3—We then sought to identify molecules that mediate the effect of PSA on tumorigenesis and metastasis of mouse melanoma cells. The *in vivo* down-regulation of HDAC3 exerted a negative effect on enhanced tumorigenic potential of B16F1 cells by PSA (Fig. 4*A*). Cytokine array analysis of sera of BALB/c mice showed that PSA induced the expression of MCP1 in an HDAC3-dependent manner (Fig. 4*B*). MCP1 is required for mast cell-mediated allergic conjunctivitis (34). The enhanced tumorigenic potential of B16F1 cells

Downloaded from http://www.jbc.org/ at Università degli Studi di Roma on June 18, 2017

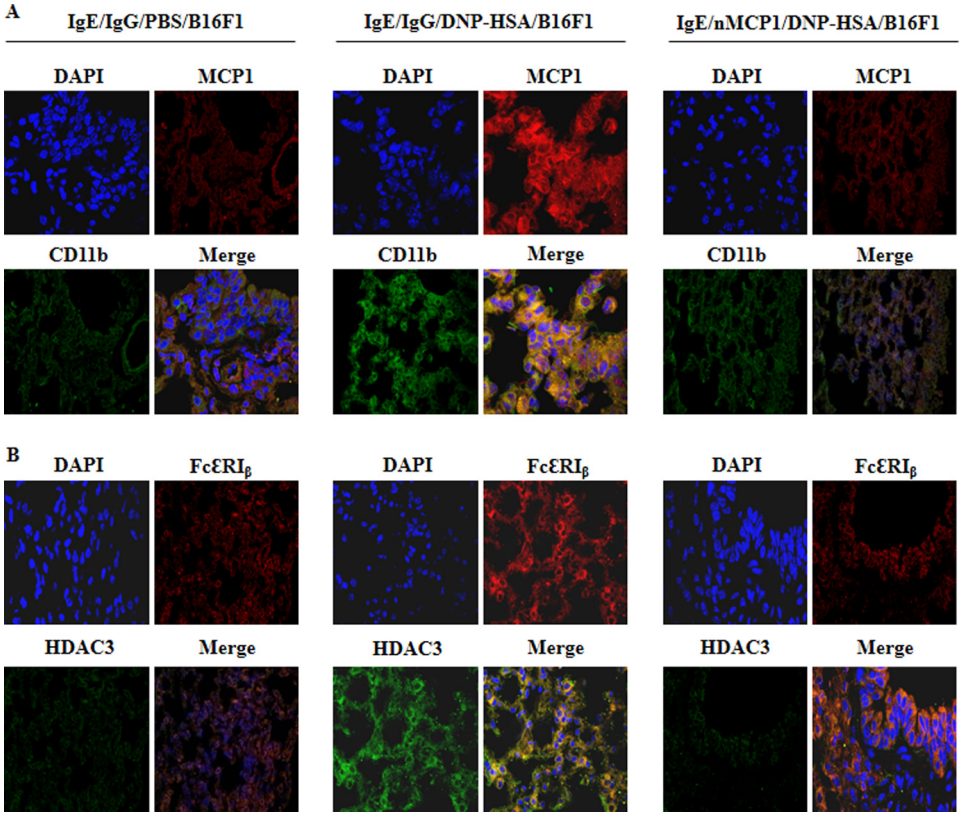

FIGURE 7. **Enhanced metastatic potential of B16F1 melanoma cells is associated with the recruitment of macrophages and the activation of mast cells.** *A,* lung tumor tissue was resected from each experimental group of mice as indicated. Cryosections were prepared, and immunofluorescence staining employing MCP1 or C11b was performed. DAPI staining was also performed for nuclear staining. *B,* same as *A* except that immunofluorescence staining employing HDAC3 or $Fc\varepsilon RI_{\beta}$ was performed.

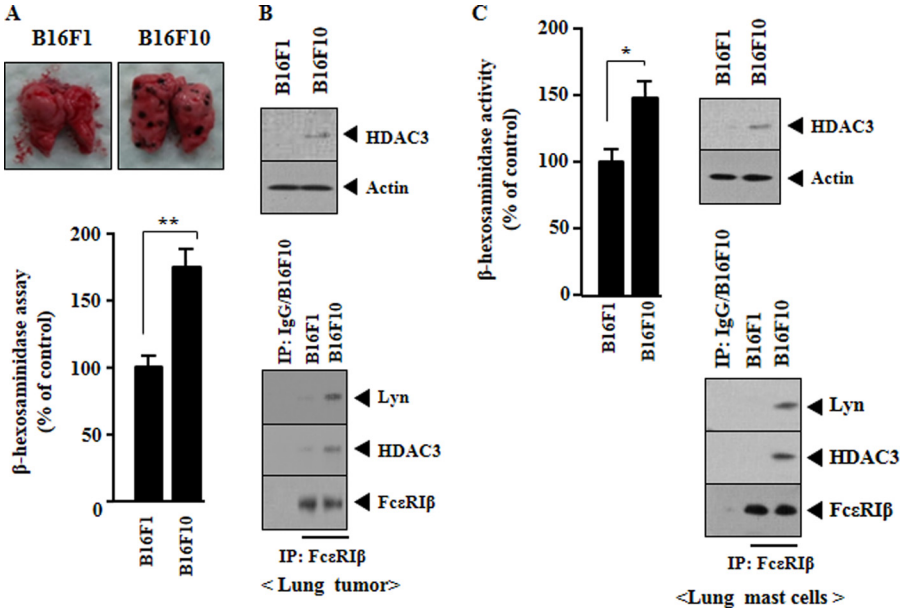

FIGURE 8. **Mouse melanoma cells activate mast cells.** *A,* BLAB/c mice were given an i.v. injection of B16F1 (10^6) or B16F10 cells (10^6). Fourteen days after the injection of tumor cells, the extent of lung metastasis was determined as described. β-Hexosaminidase activity assays using lung tumor tissue lysates were performed (*lower panel*). **, $p < 0.005$. *B,* tissue lysates from the lung tumor tissue derived from B16F1 or B16F10 were immunoprecipitated (*IP*) with the indicated antibody, followed by Western blot analysis (*lower panel*). The same tissue lysates were also subjected to Western blot analysis (*upper panel*). *C,* mast cells were isolated from the indicated lung tumor tissue and β-hexosaminidase activity assays (*left panel*). Lysates prepared from lung mast cells were immunoprecipitated with the indicated antibody, followed by Western blot analysis (*lower panel*). The same lysates were also subjected to Western blot analysis (*upper panel*).*, $p < 0.05$.

Downloaded from http://www.jbc.org/ at Università degli Studi di Roma on June 18, 2017

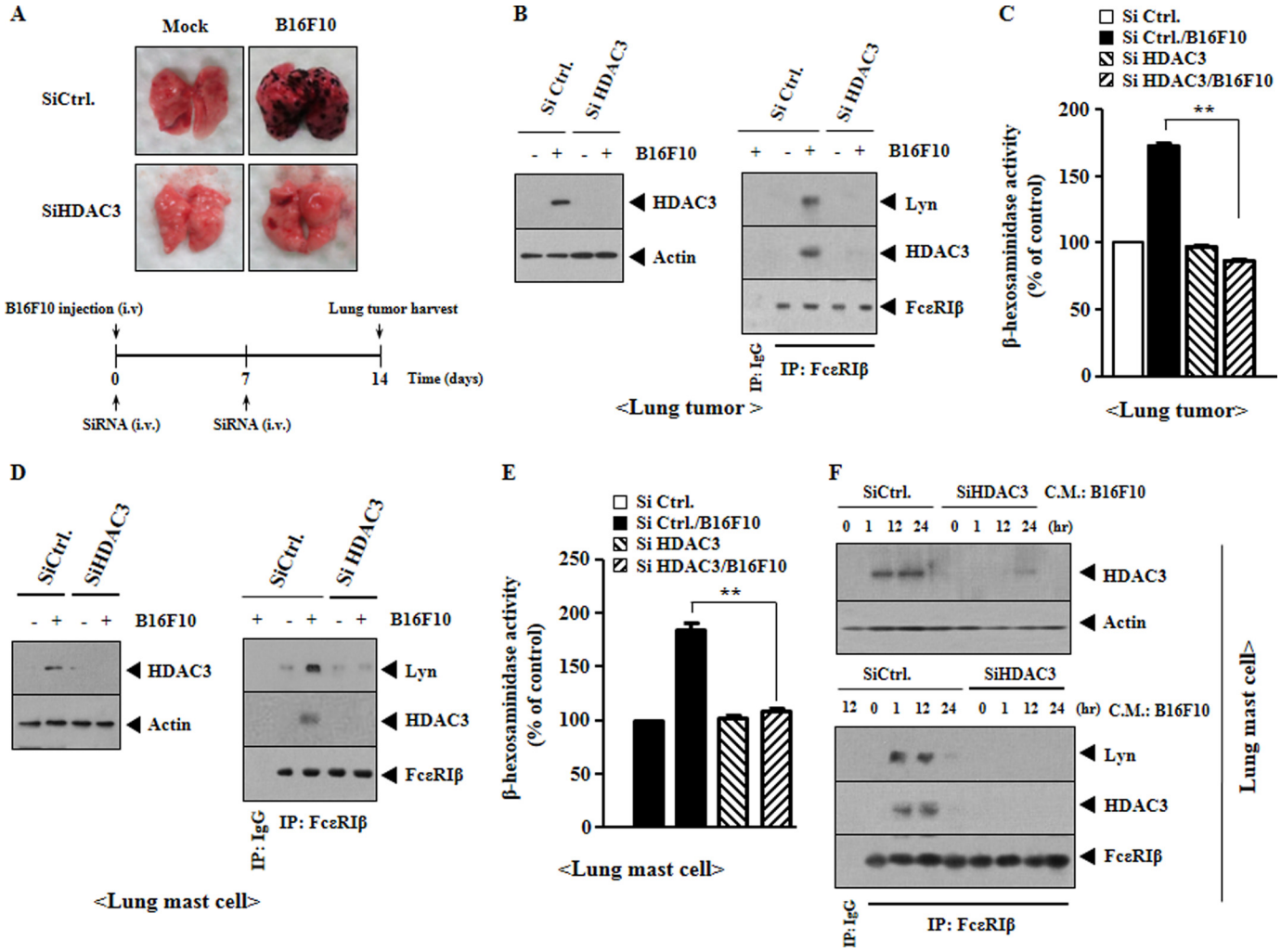

FIGURE 9. **HDAC3 is necessary for the activation of mast cells by B16F10 melanoma cells.** *A,* BALB/c mice were given an i.v. injection of B16F10 cells (2×10^5). BALB/c mice were also given an i.v. injection of Sicontrol (100 nM) or SiHDAC3 (100 nM) on the same day. Seven days after the injection of B16F10 cells, BALB/c mice were given an i.v. injection of Sicontrol (100 nM) or SiHDAC3 (100 nM). Fourteen days after the injection of B16F10 cells, the extent of lung metastasis was determined. *B,* tissue lysates from the lung tumor tissue derived from B16F10 cells were immunoprecipitated (*IP*) with the indicated antibody, followed by Western blot analysis (*right panel*). The same tissue lysates were also subjected to Western blot analysis (*left panel*). *C,* tissue lysates from the lung tumor tissue derived from B16F10 cells were subjected to β-hexosaminidase activity assays. **, $p < 0.005$. *D,* lysates from lung mast cells were immunoprecipitated with the indicated antibody (2 μg/ml), followed by Western blot analysis (*right panel*). The same cell lysates were subjected to Western blot analysis (*left panel*). *E,* mast cells were isolated from the indicated lung tumor tissue, and β-hexosaminidase activity assays were performed. **, $p < 0.005$. *F,* B16F10 cells were transiently transfected with scrambled siRNA (100 nM) or HDAC3 siRNA (100 nM). 48 h after transfection, the conditioned medium (*C.M.*) was added to lung mast cells isolated from BALB/c mouse. At each time point after addition of conditioned medium, cell lysates were isolated and subjected to Western blot analysis.

is correlated with the activation of FcεRI signaling, which involves an interaction of $Fc\epsilon RI_\beta$ with HDAC3 and Lyn (Fig. 4*C*). PSA induced the expression of MCP1, CCR2 (a receptor for MCP1), and c-Kit, a mast cell marker, in an HDAC3-dependent manner (Fig. 4*C*). ChIP assays showed that the HDAC3 binds to MCP1 promoter sequences (Fig. 4*D*), suggesting that MCP1 is a direct target of HDAC3. Taken together, these results imply that MCP1, along with HDAC3, may play a role in the PSA-mediated promotion of the tumorigenic and metastatic potential of mouse melanoma cells.

MCP1 Is Necessary for PSA-mediated Metastasis—Because MCP1 is directly regulated by HDAC3 (Fig. 4*D*), we examined the effect of MCP1 on enhanced metastatic potential of mouse melanoma cells by PSA. Neutralizing MCP1 antibody (nMCP1) prevented PSA from enhancing the metastatic potential of B16F1 cells (Fig. 5*A*). MCP1 was necessary for the induction of HDAC3, c-Kit, and CCR2 by PSA in lung tumor tissue (Fig. 5*B*, *left panel*). The fact that MCP1 regulates the expression of HDAC3 suggests that the MCP1/CCR2 signaling axis forms a feedback loop with HDAC3. The induction of HDAC3-$Fc\epsilon RI_\beta$ and $Fc\epsilon RI_\beta$-Lyn interactions by PSA in lung tumor tissue occurred in an MCP1-dependent manner (Fig. 5*B*, *right panel*). Treatment of cells with mouse recombinant MCP1 protein enhanced the metastatic potential of B16F1 cells (Fig. 5*C*). Immunohistochemical staining showed the induction of c-Kit by MCP1 treatment (Fig. 5*C*), suggesting that MCP1 induces the activation of mast cells in tumor tissue. Recombinant MCP1 protein induced its own expression (Fig. 5*C*), suggesting that MCP1 regulates its own expression through CCR2. Western blotting analysis of lung tumor tissue lysates showed the induction of HDAC3, Snail, and CCR2 by MCP1 protein (Fig. 5*D*). Taken together, these results suggest that the MCP1/CCR2 sig-

Downloaded from http://www.jbc.org/ at Università degli Studi di Roma on June 18, 2017

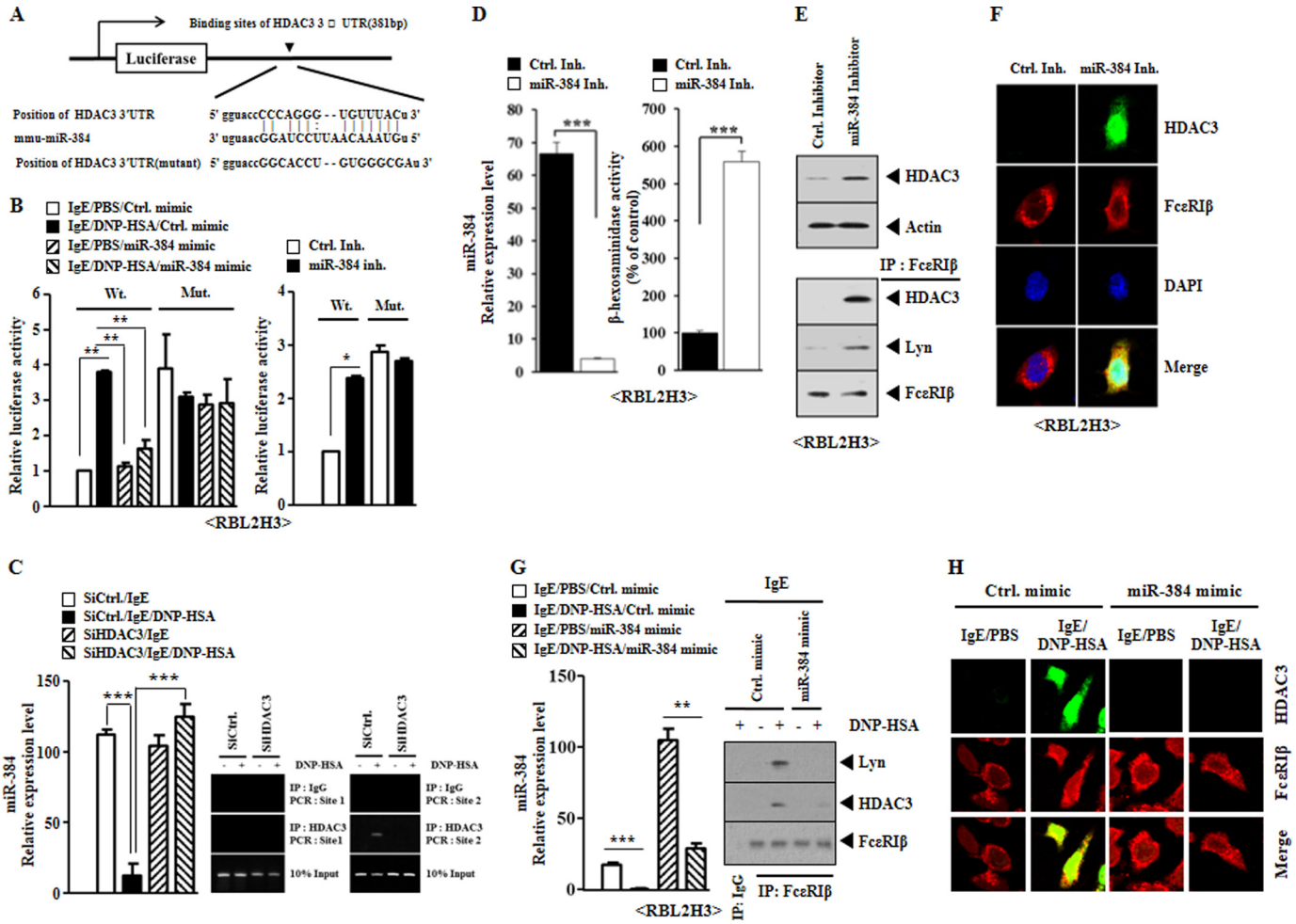

FIGURE 10. **miR-384 acts as a negative regulator of HDAC3 and *in vitro* allergic inflammation.** *A* shows the potential binding of miR-384 to 3′-UTR-HDAC3. *B*, RBL2H3 cells were transfected with control mimic (10 nM) or miR-384 mimic (10 nM) along with wild type Luc-HDAC3–3′-UTR or mutant (*mut*) Luc-HDAC3–3′-UTR. The next day, cells were sensitized with DNP-specific IgE (100 ng/ml) for 24 h, followed by stimulation with DNP-HSA (100 ng/ml) for 1 h. Luciferase activity assays were performed as described. *, $p < 0.05$; **, $p < 0.005$. *C*, RBL2H3 cells were transfected with scrambled siRNA (10 nM) or HDAC3 siRNA (10 nM). The next day, cells were sensitized with DNP-specific IgE (100 ng/ml) for 24 h, followed by stimulation with DNP-HSA (100 ng/ml). One hour after DNP-HSA stimulation, miRNAs were isolated, and the expression of miR-384 was determined by quantitative real time PCR (*left panel*). ChIP assays were performed to examine binding of HDAC3 to the promoter sequences of miR-384 (*right panel*). Numbers in *parentheses* denote putative binding sites for transcription factors in the promoter sequences of miR-384. ***, $p < 0.0005$. *D*, RBL2H3 cells were transfected with control inhibitor (*Ctrl. Inh*) (10 nM) or miR-384 inhibitor (10 nM). The next day, miRNAs were isolated, and the expression of miR-384 was determined by quantitative real time PCR (*left panel*). Cell lysates were subjected to β-hexosaminidase activity assays were performed (*right panel*). *E*, same as *D* except that Western blot and immunoprecipitation were performed. *F*, same as *D* except that immunofluorescence staining was performed. *G*, RBL2H3 cells were transfected with control mimic (10 nM) or miR-384 mimic (10 nM). The next day, cells were sensitized with DNP-specific IgE (100 ng/ml) for 24 h, followed by stimulation with DNP-HSA (100 ng/ml). One hour after DNP-HSA stimulation, miRNAs were isolated, and the expression of miR-384 was determined by quantitative real time PCR (*left panel*). Cell lysates were also prepared and subjected to immunoprecipitation with the indicated antibody (2 μg/ml), followed by Western blot analysis (*right panel*). **, $p < 0.005$; ***, $p < 0.0005$. *H*, RBL2H3 cells were transfected with control mimic (10 nM) or miR-384 mimic (10 nM). The next day, cells were sensitized with DNP-specific IgE (100 ng/ml) for 24 h, followed by stimulation with DNP-HSA (100 ng/ml) for 1 h. Immunofluorescence staining was performed as described.

naling axis mediates enhanced metastatic potential of mouse melanoma cells by PSA.

MCP1 Is Necessary for the Enhanced Invasion and Migration Potential of Tumor Cells by Allergic Inflammation—MCP1 was necessary for the enhanced metastatic potential of B16F1 cells (Fig. 5*A*); based on these data, we hypothesized that MCP1 might enhance migration and invasion of tumor cells. Cytokine array analysis showed the induction of MCP1 in antigen-stimulated RBL2H3 cells and increased expression and phosphorylation of CCR2 in antigen-stimulated RBL2H3 cells (Fig. 6, *A* and *B*). The conditioned medium of antigen-stimulated RBL2H3 cells or BMMCs induced the expression of HDAC3, MCP1, and CCR2 in B16F1 cells (Fig. 6*C*). However, the conditioned medium of RBL2H3 cells transfected with siHDAC3 did not induce expression of HDAC3, MCP1, or CCR2 in B16F1 cells (Fig. 6*C*). Moreover, the conditioned medium of BMMCs or RBL2H3 cells treated with neutralizing MCP1 antibody did not induce expression of HDAC3, MCP1, or CCR2 in B16F1 cells (Fig. 6*C*). These results suggest that HDAC3 and MCP1 mediate the interaction between mouse mast and melanoma cells. The conditioned medium of antigen-stimulated RBL2H3 or BMMCs enhanced the migration potential of B16F1 cells, and this enhanced migration potential was dependent on MCP1 (Fig. 6*D*). The conditioned medium of antigen-stimulated RBL2H3 or BMMCs enhanced the invasion potential of B16F1 cells, and this enhanced invasion potential was depen-

Downloaded from http://www.jbc.org/ at Università degli Studi di Roma on June 18, 2017

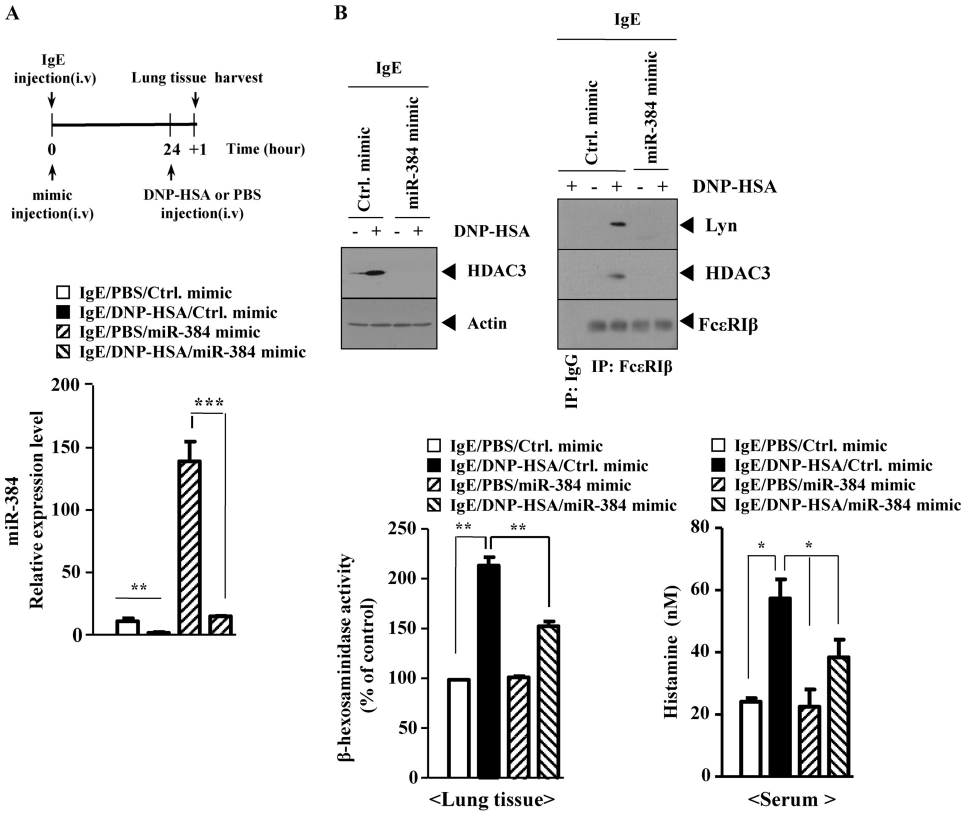

FIGURE 11. **miR-384 acts as a negative regulator of PSA.** *A*, BALB/c mice were sensitized to DNP-specific IgE (0.5 μg/kg) by an i.v. injection. BALB/c mice were also given an i.v. injection of control mimic (100 nM) or miR-384 mimic (100 nM). The next day, BALB/c mice were given an i.v. injection of DNP-HSA (250 μg/kg). One hour after stimulation with DNP-HSA, lung tissues were isolated and the expression of miR-384 was determined by quantitative real time PCR. **, $p < 0.005$; ***, $p < 0.0005$. *B*, same as *A* except that immunoprecipitation, Western blot, and β-hexosaminidase activity assays were performed. For histamine release assays, sera of BALB/c mice were employed. *, $p < 0.05$; **, $p < 0.005$.

dent on MCP1 (Fig. 6*E*). Taken together, these results suggest that MCP1 exerts paracrine control over tumor cells to enhance their invasion and migration potential.

PSA Induces the Recruitment of Macrophages to Tumor Tissues and Activation of Mast Cells by MCP1—Macrophages play essential role in tumor metastases (35). In our mouse model of PSA, there was increased expression of MCP1 and CD11b, a marker of macrophages, in lung tumor tissues (Fig. 7*A*, *middle panels*). In addition, PSA induced co-localization of MCP1 with CD11b (Fig. 7*A*, *middle panels*), suggesting that MCP1 recruits macrophages to promote tumor metastasis. MCP1 was responsible for the increased expression of CD11b (Fig. 7*A*, *right panels*). PSA induced the expression of HDAC3 and the co-localization of FcϵRI$_\beta$ with HDAC3 (Fig. 7*B*, *middle panels*), both of which were dependent on MCP1 (Fig. 7*B*, *right panels*). Taken together, these results suggest that MCP1 is necessary for the recruitment of macrophages for creation of a tumor microenvironment that leads to enhanced tumor metastasis.

Tumor Cells Induce Activation of Mast Cells—We then examined whether there is a positive feedback regulatory loop between allergic inflammation and tumor metastasis. We tested this hypothesis by assessing whether tumor cells would activate mast cells. When injected into BALB/c mouse, B16F10 cells showed higher metastatic potential than B16F1 cells (Fig. 8*A*). Lung tumor tissue derived from B16F10 cells showed higher β-hexosaminidase activity and HDAC3 expression, along with an increased interaction between FcϵRI$_\beta$, Lyn, and HDAC3 than those derived from B16F1 cells (Fig. 8, *A* and *B*). Mast cells isolated from lung tumor tissue derived from B16F10 cells showed higher β-hexosaminidase activity, HDAC3 expression, and an increased interaction between FcϵRI$_\beta$, Lyn, and HDAC3 than those derived from B16F1 cells (Fig. 8*C*). Taken together, these results suggest the presence of a positive feedback loop between tumor and mast cells.

HDAC3 Is Necessary for the Activation of Mast Cells by Tumor Cells—The fact that tumor cells activate mast cells led us to examine the involvement of HDAC3 in this process. B16F10 cells showed higher metastatic potential than B16F1 cells (Fig. 9*A*). The *in vivo* down-regulation of HDAC3 decreased the metastatic potential of B16F10 cells (Fig. 9*A*). Western blotting analysis of lung tumor tissue lysates showed that the down-regulation of HDAC3 prevented the interaction between FcϵRI$_\beta$ and HDAC3 (Fig. 9*B*). The *in vivo* down-regulation of HDAC3 also decreased β-hexosaminidase activity associated with lung tumor tissue (Fig. 9*C*) and prevented an interaction between FcϵRI$_\beta$ and HDAC3 in lung mast cells derived from lung tumor tissue derived from B16F10 cells (Fig. 9*D*). The conditioned medium of B16F10 cells increased β-hexosaminidase activity in lung mast cells (Fig. 9*E*). However, the conditioned medium of B16F10 cells transfected with HDAC3 siRNA did not affect β-hexosaminidase activity in lung mast cells or promote the formation of the FcϵRI$_\beta$-HDAC3 complex in lung mast cells (Fig. 9, *E* and *F*). Taken together, these results suggest that tumor cells induce the

Downloaded from http://www.jbc.org/ at Università degli Studi di Roma on June 18, 2017

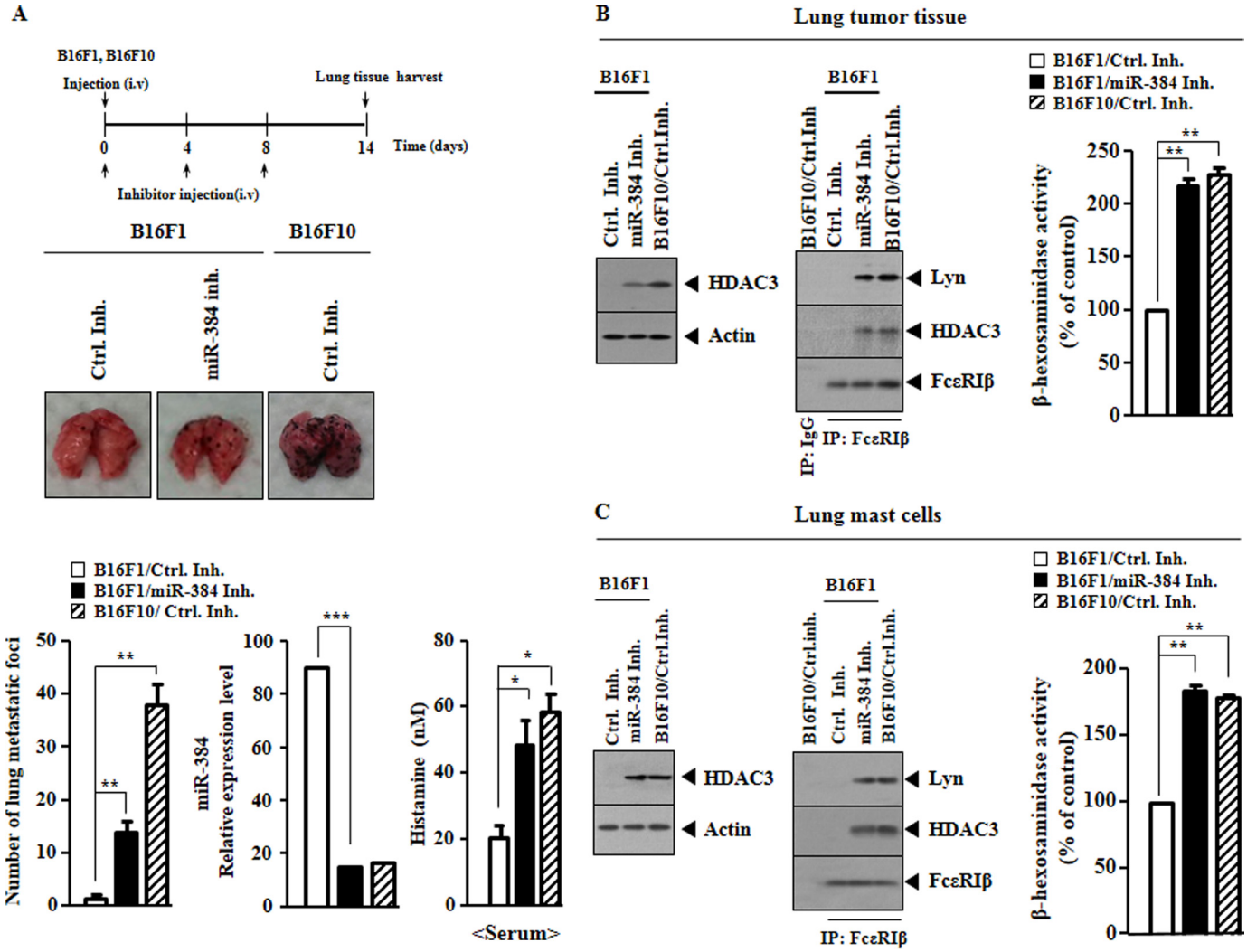

FIGURE 12. **miR-384 inhibitor enhances the metastatic potential and mast cell activation by tumor cells.** *A,* BALB/c mice were given an i.v. injection with B16F1 (2×10^5) or B16F10 cells (2×10^5). BALB/c mice were given an i.v. injection with control inhibitor (100 nM) or miR-384 inhibitor (100 nM) on the day 0, 4, and 8 of the time line. Fourteen days after the injection of B16F1 or B16F10 cells, the extent of lung metastasis was determined. miRNA from each mouse of each experimental group was isolated, and the expression of miR-384 was determined by quantitative real time PCR. Histamine release assays employing sera of BALB/c mice were also performed. *, $p < 0.05$; **, $p < 0.005$. ***, $p < 0.0005$. *B,* lysates from lung tumor tissue of each experimental group were immunoprecipitated with the indicated antibody (2 μg/ml), followed by Western blot (*middle panel*). Lysates were subjected to Western blot analysis (*left panel*). Lysates were subjected to β-hexosaminidase activity assays were performed (*right panel*). **, $p < 0.005$. *C,* same as *B* except that lung mast cells isolated from lung tumor tissue were employed. **, $p < 0.005$.

activation of mast cells through the HDAC3/MCP1/CCR2 signaling axis.

miR-384 Acts as a Negative Regulator of HDAC3 and Allergic Inflammation—The role of miRNAs in allergic inflammation and an interaction between tumor cells and mast cells remain largely unknown. Target scan analysis predicted the binding of miR-384 to the 3′-UTR of HDAC3 (Fig. 10*A*). The miR-384 mimic decreased luciferase activity of the 3′-wild type UTR-HDAC3 but not luciferase activity of the mutant 3′-UTR-HDAC3 (Fig. 10*B*). Antigen stimulation decreased the expression of miR-384 (Fig. 10*C*). The down-regulation of HDAC3 restored the expression of miR-384 in antigen-stimulated RBL2H3 cells (Fig. 10*C*). We examined whether HDAC3 directly regulates the expression of miR-384. miR-384 promoter sequences contain putative binding sites for various transcription factors, such as HDAC3, HDAC2, SOX-5, and HSF (Fig. 10*C*). HDAC3 showed binding to the promoter sequences of miR-384 that contain a putative binding site for HDAC3 (Fig. 10*C*).

These results suggest that miR-384 and HDAC3 form a feedback regulatory loop. The miR-384 inhibitor increased β-hexosaminidase activity in RBL2H3 cells (Fig. 10*D*). The miR-384 inhibitor induced an interaction between $Fc\epsilon RI_\beta$ and HDAC3, increased the expression of HDAC3, and induced co-localization of HDAC3 with $Fc\epsilon RI_\beta$ in RBL2H3 cells (Fig. 10, *E* and *F*). The miR-384 mimic prevented an interaction between $Fc\epsilon RI_\beta$ and HDAC3 in antigen-stimulated RBL2H3 cells, decreased the expression of HDAC3, and prevented co-localization of HDAC3 with $Fc\epsilon RI_\beta$ (Fig. 10, *G* and *H*). Taken together, these results suggest that miR-384 acts as a negative regulator of HDAC3 and allergic inflammation.

miR-384 Acts as a Negative Regulator of PSA—We employed the BALB/c mouse model of PSA to examine the *in vivo* role of miR-384. PSA decreased the expression of miR-384 (Fig. 11*A*).

Downloaded from http://www.jbc.org/ at Università degli Studi di Roma on June 18, 2017

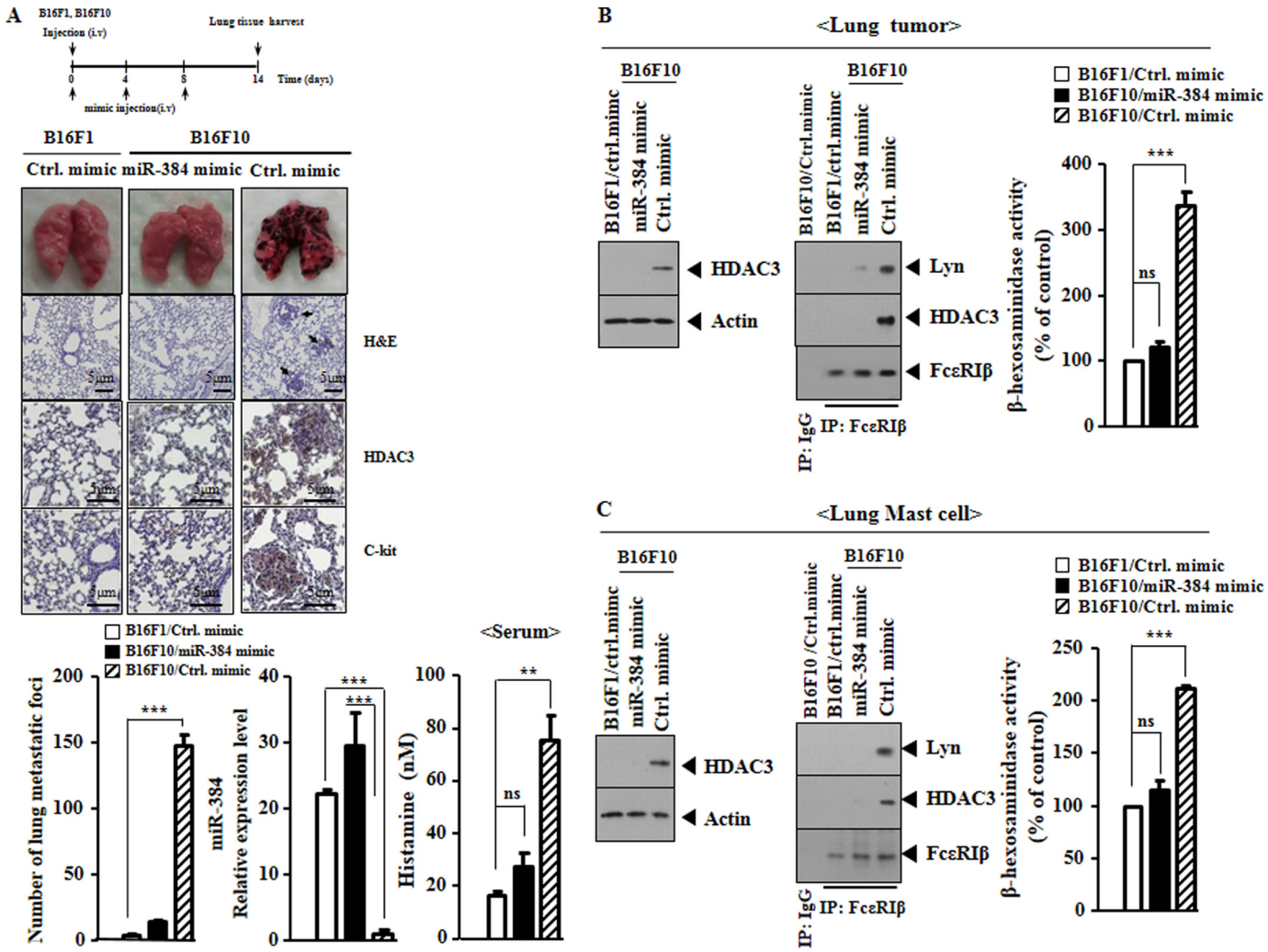

FIGURE 13. **miR-384 mimic negatively regulates the enhanced metastatic potential and mast cell activation by tumor cells.** *A*, BALB/c mice were given an i.v. injection with B16F1 (2×10^5) or B16F10 cells (2×10^5). BALB/c mice were given an i.v. injection with control mimic (100 nM) or miR-384 mimic (100 nM) on the days 0, 4, and 8 of the time line. Fourteen days after the injection of B16F1 or B16F10 cells, the extent of lung metastasis was determined. miRNA from each mouse of each experimental group was isolated, and the expression of miR-384 was determined by quantitative real time PCR. Formalin-fixed lung sections were stained with H&E. *Black arrows* indicate lung metastatic foci (*scale bar*, 5 μm). Immunohistochemical staining employing lung tumor tissue was performed as described. Histamine release assays employing sera of BALB/c mice were also performed. **, $p < 0.005$; ***, $p < 0.0005$; *ns*, not significant. *B*, lysates from lung tumor tissue of each experimental group were immunoprecipitated (*IP*) with the indicated antibody (2 μg/ml), followed by Western blot (*middle panel*). Lysates were subjected to Western blot analysis (*left panel*). Lysates were subjected to β-hexosaminidase activity assays were performed (*right panel*). ***, $p < 0.005$; *ns*, not significant. *C*, same as *B* except that lung mast cells isolated from lung tumor tissue were employed. ***, $p < 0.005$; *ns*, not significant.

Western blotting analysis of lung tissue showed that the miR-384 mimic attenuated the antigen-stimulated increase in HDAC3 expression and prevented an interaction between HDAC3 and FcϵRI$_\beta$ in lung tissue, along with inhibiting β-hexosaminidase activity associated with the mouse model of PSA (Fig. 11*B*). PSA increased the secretion of histamine, which was attenuated by treatment with the miR-384 mimic (Fig. 11*B*). Taken together, these results suggest that miR-384 is a negative regulator of PSA.

miR-384 Inhibitor Enhances Metastatic Potential of Tumor Cells—Next, we examined whether miR-384 affects the metastatic potential of tumor cells. B16F10 cells showed higher metastatic potential than B16F1 cells, and treatment with an miR-384 inhibitor enhanced the metastatic potential of B16F1 cells (Fig. 12*A*) and decreased the expression of miR-384 in lung tumor tissue (Fig. 12*A*). BALB/c mice injected with B16F10 cells showed higher secretion levels of histamine than those injected with B16F1 cells (Fig. 12*A*). Treatment with an miR-384 inhibitor increased the secretion of histamine in sera of BALB/c mice injected with B16F1 cells (Fig. 12*A*). Western blotting analysis of lung tumor tissue showed that treatment with an miR-384 inhibitor increased the expression of HDAC3 and induced an interaction between HDAC3 and FcϵRI$_\beta$, while also increasing the β-hexosaminidase activity in lung tumor tissue (Fig. 12*B*). Western blotting analysis of lung mast cells from lung tumor tissue derived from B16F1 cells showed that miR-384 increased the expression of HDAC3 and induced an interaction between HDAC3 and FcϵRI$_\beta$, while also increasing β-hexosaminidase activity in lung mast cells derived from lung tumor tissue derived from B16F1 cells (Fig. 12*C*). Taken together, these results suggest that miR-384 negatively regulates the metastatic potential of B16F1 cells by regulating the expression of HDAC3.

Downloaded from http://www.jbc.org/ at Università degli Studi di Roma on June 18, 2017

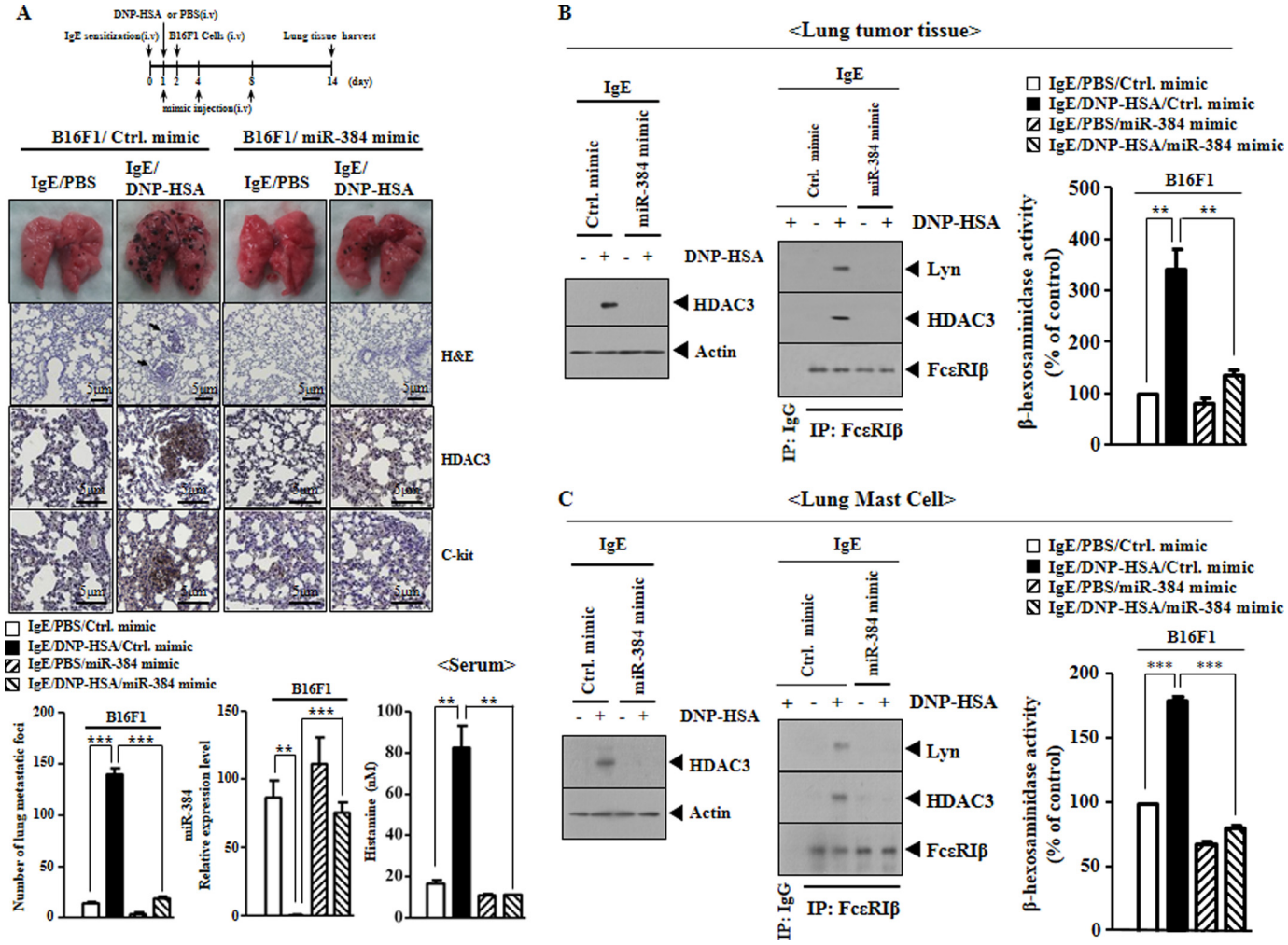

FIGURE 14. **miR-384 negatively regulates the enhanced metastatic potential of tumor cells by PSA.** *A*, BALB/c mice were sensitized to DNP-specific IgE (0.5 μg/kg) by an i.v. injection. The next day, BALB/c mice were given an i.v. injection of DNP-HSA (250 μg/kg). Each mouse received injection of B16F1 melanoma cells (2×10^5) on day 2 of the time line. BALB/c mice were given an i.v. injection with control mimic (100 nM) or miR-384 mimic (100 nM) on days 4 and 8 of the time line. Fourteen days after the injection of B16F1 cells, the extent of lung metastasis was determined. miRNA from each mouse of each experimental group was isolated, and the expression of miR-384 was determined by quantitative real time PCR. Formalin-fixed lung sections were stained with H&E. *Black arrowheads* indicate lung metastatic foci. (*Scale bar*, 5 μm.) Immunohistochemical staining employing lung tumor tissue was performed as described. Histamine release assays employing sera of BALB/c mice were performed. **, $p < 0.005$; ***, $p < 0.005$. *B*, lysates from lung tumor tissue of each experimental group were immunoprecipitated (*IP*) with the indicated antibody (2 μg/ml), followed by Western blot (*middle panel*). Lysates were subjected to Western blot analysis (*left panel*). Lysates were subjected to β-hexosaminidase activity assays (*right panel*). **, $p < 0.05$. *C*, same as *B* except that lung mast cells isolated from lung tumor tissue were employed. ***, $p < 0.005$.

miR-384 Mimic Decreases Metastatic Potential of Tumor Cells—We next examined whether overexpression of miR-384 would negatively regulate the metastatic potential of tumor cells. Treatment with the miR-384 mimic decreased the metastatic potential of B16F10 cells and decreased the expression of HDAC3 in lung tumor tissue (Fig. 13*A*). Moreover, the miR-384 mimic decreased the expression of c-kit, a marker of mast cell activation (Fig. 13*A*), suggesting the activation of mast cells by B16F10 cells. Histological analysis confirmed that B16F10 cells generated not only more but also significantly larger metastatic foci in the BALB/c mice than B16F1 cells, with B16F10/miR-384 mimic reducing the metastatic burden (Fig. 13*A*). The miR-384 mimic decreased the secretion of histamine in sera of BALB/c mice injected with B16F10 cells (Fig. 13*A*). Western blotting analysis of lung tumor tissue showed that miR-384 mimic decreased the expression of HDAC3 and inhibited an interaction between HDAC3 and FcϵRI$_\beta$ (Fig. 13*B*), along with decreasing the β-hexosaminidase activity in lung tumor tissue (Fig. 13*B*). Western blotting analysis of lung mast cells from lung tumor tissue derived from B16F10 cells showed that miR-384 mimic decreased the expression of HDAC3 and inhibited an interaction between HDAC3 and FcϵRI$_\beta$ (Fig. 13*C*), along with decreasing β-hexosaminidase activity in lung mast cells (Fig. 13*C*). Taken together, these results suggest that miR-384 negatively regulates metastatic potential by decreasing the expression of HDAC3.

miR-384 Attenuates the PSA-mediated Enhancements of Metastatic Potential—Treatment with an miR-384 mimic negatively attenuated the PSA-mediated effects on B16F1 cell metastasis, decreased the expression of HDAC3 in lung tumor tissue derived from B16F1 cells, and decreased the expression of c-kit, a marker of mast cell activation (Fig. 14*A*). In addition, treatment with the miR-384 mimic attenuated the PSA-mediated increase in the number of metastatic foci and histamine

Downloaded from http://www.jbc.org/ at Università degli Studi di Roma on June 18, 2017

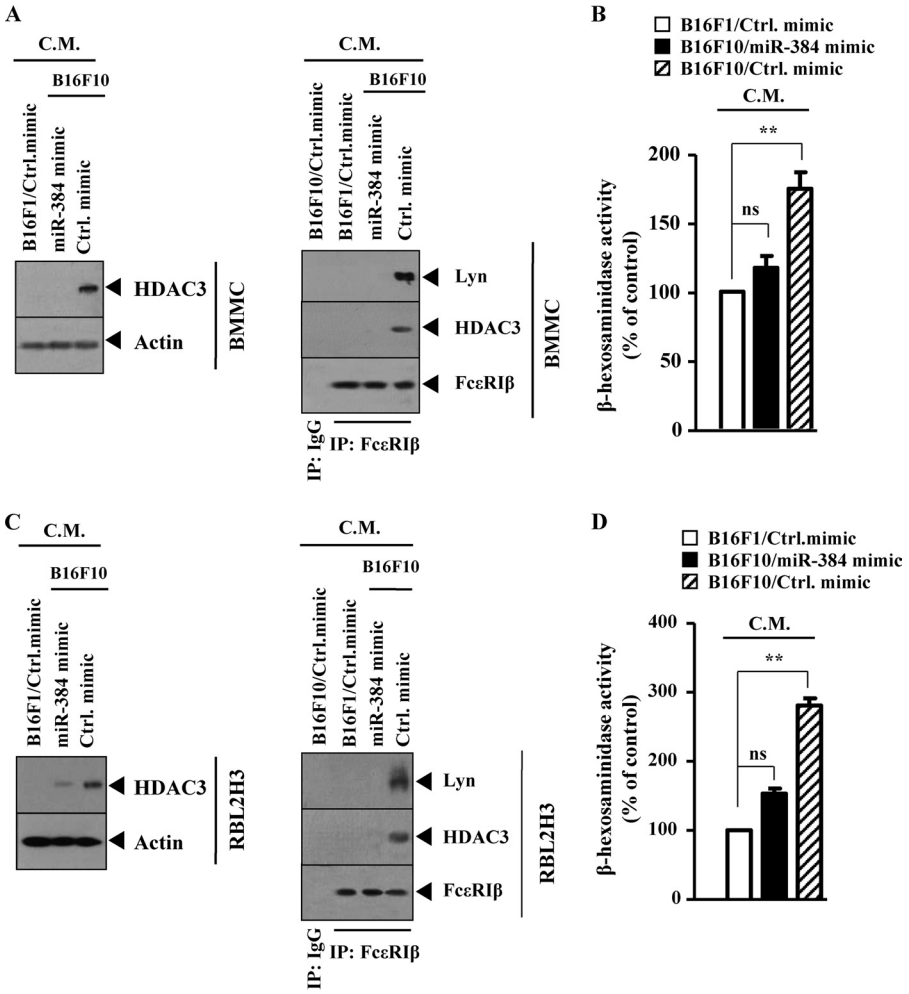

FIGURE 15. **miR-384 exerts a negative regulation on the interaction between tumor cells and mast cells.** *A,* B16F1 or B16F10 cells were transfected with control mimic (10 nM) or miR-384 mimic (10 nM). At 48 h after transfection, the conditioned medium (*C.M.*) was added to BMMC. Twelve hours after addition of conditioned medium, cell lysates were immunoprecipitated (*IP*) with the indicated antibody (2 μg/ml), followed by Western blot analysis. Cell lysates were also subjected to Western blot analysis. *B,* same as *A* except that β-hexosaminidase activity assays were performed. **, $p < 0.005$; *ns*, not significant. *C,* same as *A* except that the conditioned medium was added to RBL2H3 cells. **, $p < 0.005$; *ns*, not significant. *D,* same as *B* except that RBL2H3 cells were employed.

secretion in sera of BALB/c mice (Fig. 14*A*). Western blotting analysis of lung tumor tissue showed that the miR-384 mimic treatment decreased the expression of HDAC3, inhibited an interaction between HDAC3 and FcϵRI$_\beta$, and decreased β-hexosaminidase activity in lung tumor tissue (Fig. 14*B*). Western blotting analysis of lung mast cell lysates from lung tumor tissue derived from B16F1 cells showed that the miR-384 mimic decreased the expression of HDAC3, inhibited an interaction between HDAC3 and FcϵRI$_\beta$, and decreased β-hexosaminidase activity in lung mast cells (Fig. 14*C*). Taken together, these results confirm that miR-384 attenuated the effects of PSA on metastasis by decreasing the expression of HDAC3.

miR-384 Regulates the Interaction between Tumor Cells and Mast Cells—The conditioned medium of B16F10 cells induced the expression of HDAC3 in BMMCs and RBL2H3 cells (Fig. 15, *A* and *C*). The conditioned medium of B16F10 cells transfected with miR-384 mimic did not induce the expression of HDAC3 in BMMCs or RBL2H3 cells (Fig. 15, *A* and *C*). The conditioned medium of B16F1 cells did not induce the expression of HDAC3 in BMMCs or RBL2H3 cells (Fig. 15, *A* and *C*). Furthermore, the conditioned medium of B16F10 cells increased β-hexosaminidase activity in BMMCs and RBL2H3 cells (Fig. 15*D*), and these effects were reversed with treatment from the miR-384 mimic (Fig. 15, *B* and *D*). Taken together, these results suggest that miR-384 may regulate the positive feedback relationship between tumor and mast cells.

DISCUSSION

We previously reported the induction of HDAC3 and the decreased expression of E-cadherin in antigen-stimulated RBL2H3 cells (30). HDAC3 represses the expression of E-cadherin (36), a protein involved in EMT. Hypoxia-inducible factor-1α-mediated HDAC3 expression is essential for hypoxia-induced EMT and metastasis (37). Hypoxia-inducible factor promotes the murine allergic airway inflammation and is increased in asthma and rhinitis (38). These reports led us to hypothesize that HDAC3 may link allergic inflammation with tumor metastasis. HDAC3 plays an essential role in allergic skin inflammation, such as passive cutaneous anaphylaxis (23). However, the role of HDAC3 in PSA has not been reported. In

Downloaded from http://www.jbc.org/ at Università degli Studi di Roma on June 18, 2017

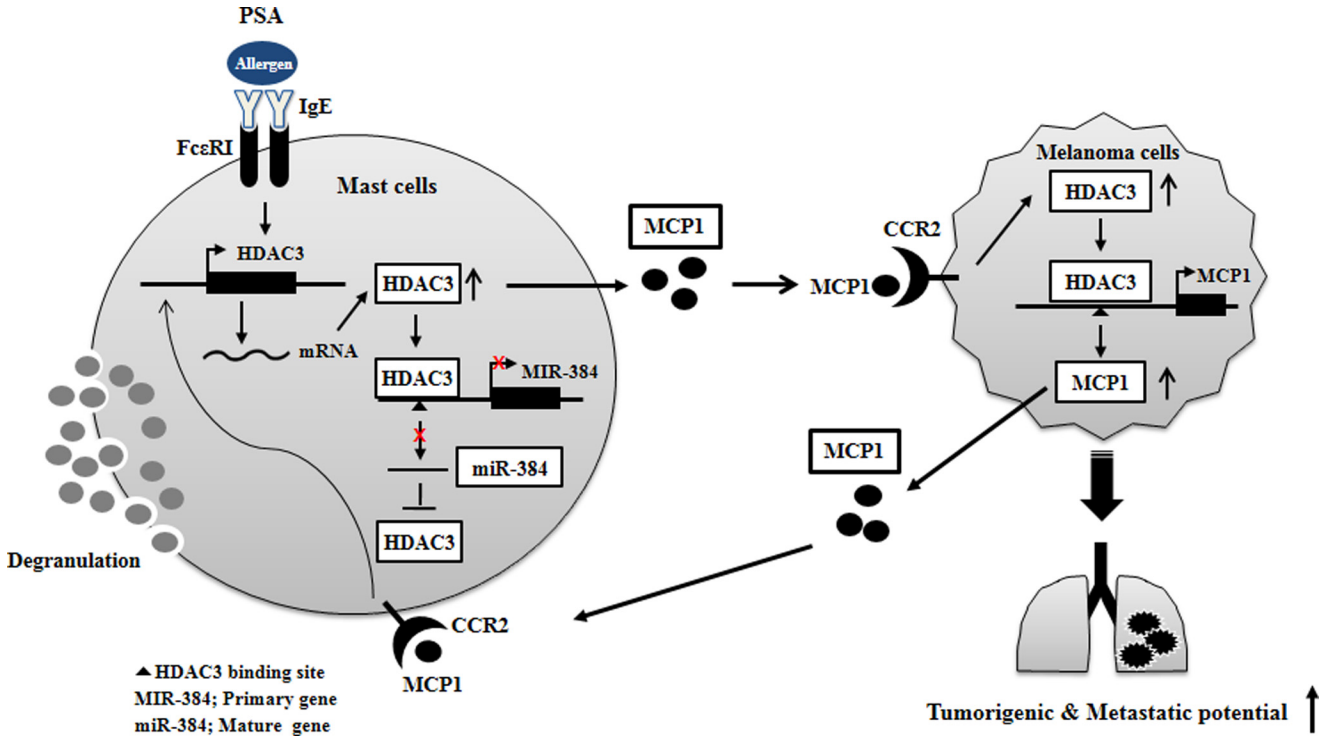

FIGURE 16. **Proposed mechanism of positive feedback relationship mediated by HDAC3.** *CCR2*, chemokine, cc motif, receptor 2; *HDAC3*, histone deacetylase-3; *MCP1*, monocyte chemoattractant protein-1; *PSA*, passive systemic anaphylaxis.

this study, we show that HDAC3 is necessary for PSA and the activation of mast cells by PSA.

The expression of integrin $\alpha5$ is increased in tumor tissue derived from B16F10 cells after PSA induction. Integrin $\alpha5$, through interaction with epidermal growth factor receptor, is necessary for allergic skin inflammation (30) and is also necessary for interaction between T cells and fibroblasts in airway inflammation (39). It is reasonable that integrin $\alpha5$ may mediate cellular interaction, if any, between mast and tumor cells. It will be interesting to examine the involvement of EGF receptor signaling in relation to FcϵRI in PSA. Because PSA induces the expression of HDAC3, it is probable that HDAC3 up-regulates the expression of integrin $\alpha5$ to induce an interaction between tumor and mast cells. Tumors derived from B16F10 cells under PSA exhibit the increased expression of VCAM-1 and integrin $\alpha4$ in our mouse model of PSA. VCAM-1, induced by Th2 cytokines, such as IL-12, contributes to allergen-induced experimental asthma (40). In the bone marrow, VCAM-1 attracts and tethers $\alpha4$ integrin-expressing osteoclast progenitors to facilitate their maturation into multinucleated osteoclasts that mediate osteolytic metastasis (41). These data imply a role for VCAM-1 in mediating an interaction between tumor and mast cells. Overall, it is reasonable to conclude that the enhancement in metastatic potential mediated by PSA involves interactions between mast and tumor cells.

Our data show that PSA induces the activation of FcϵRI signaling in lung tissue and that HDAC3 mediates PSA-promoted enhanced tumorigenic and metastatic potential. We hypothesized that mast and tumor cells would form a positive feedback loop.

Integrin $\beta5$ enhances paracrine function of angiogenic cells via activation of signal transducer and activator of transcription (STAT) and induction of MCP1 (42). We showed that tumors derived from B16F1 cells under PSA have higher MCP1 levels. HDAC3 has been shown to promote TNF-α expression (22), and TNF-α induces the expression of MCP1 via the p38 MAPK signaling pathway (43). The MCP1/CCR2 axis is involved in peritoneal dialysis-related EMT of peritoneal mesothelial cells (44). These data imply a paracrine role for MCP1 in mediating an interaction between tumor and mast cells. In this study, we demonstrate the role of MCP1 in PSA-promoted enhanced metastatic potential of B16F1 cells. The fact that MCP1 protein induces the expression of CCR2 and HDAC3 in tumor tissue derived from B16F1 cells suggests a paracrine role of MCP1 in PSA-promoted enhanced metastatic potential of tumor cells. Our data indicate that MCP1 secreted by antigen-stimulated BMMCs activates CCR2 signaling in B16F1 cells, which in turn induces the expression of HDAC3 and MCP1. Therefore, it is reasonable to conclude that mast cells exert a paracrine control over tumor cells via MCP1.

Stem cell factor-producing tumors are capable of recruiting mast cells into the tumor, which in turn promotes the expression of many factors that facilitate activation of Treg cells, thus promoting tumor growth (12). Cancer-induced expansion and activation of CD11b$^+$ Gr-1$^+$ cells predispose mice to adenovirus-triggered anaphylactoid-type (45). These reports suggest a role of tumor cells in the activation of mast cells.

Based on our observations, we hypothesized that tumor and mast cells form a positive feedback loop. We show that the conditioned medium of B16F10 cells activates FcϵRI signaling in lung mast cells in an HDAC3-dependent manner, which indicates that HDAC3 mediates an interaction between tumor and mast cells by regulating the expression of MCP1.

Downloaded from http://www.jbc.org/ at Università degli Studi di Roma on June 18, 2017

In this study, we found that PSA activated various stromal cells such as macrophages and endothelial cells, in an HDAC3-dependent manner.[4] The activated macrophages and endothelial cells, in an HDAC3-dependent manner, enhanced the invasion potential of B16F1 cells,[4] suggesting that these stromal cells, just like mast cells, contribute to the enhanced the metastatic potential of B16F1 cell by PSA. We also found a positive feedback relationship between tumor cells and these stromal cells.[4] We are currently working on the molecular mechanisms associated with the enhanced metastatic potential of B16F1 cells by macrophages and endothelial cells.

miR-221 influences effector functions and actin cytoskeleton in mast cells (46), and it acts as a positive transcriptional regulator of c-kit (47). The loss of miR-21 significantly enhances the Th1-associated delayed-type hypersensitivity cutaneous responses (18). We show that miR-384 and HDAC3 form a feedback regulatory loop and that miR-384 acts as a negative regulator of allergic inflammation and the interaction between mast and tumor cells. Further studies are necessary to further identify factor(s) regulated by miR-384, and these additional studies will improve our understanding of the role of PSA in tumorigenesis. Because miRNAs target multiple genes, studies focused on examining whether miR-384 affects expression of various genes other than HDAC3 are also warranted. In this study, we also found that the expression of miR-212 was decreased in the mouse model of PSA.[4] It would be interesting to examine the effect of miR-212 on the expression of HDAC3 and the interaction between tumor and mast cells.

Just like other HDACs, HDAC3 may have broad effects on chromatin. Although we identified MCP1 as a target of HDAC3, it would be challenging to attribute a positive feedback relationship between anaphylaxis and tumor to HDAC3/MCP1/CCR2 axis alone. Therefore, it would be necessary to identify miRNA genes and downstream genes that are regulated by HDAC3 for better understanding of the mechanism of PSA-promoted tumor metastasis.

In this study, we show that the miR-384/HDAC3 axis regulates a positive feedback relationship between tumor and mast cells (Fig. 16). Thus, HDAC3 can be developed as a therapeutic target in treatment of allergic inflammation and cancer.

REFERENCES

1. Taranova, A. G., Maldonado, D., 3rd, Vachon, C. M., Jacobsen, E. A., Abdala-Valencia, H., McGarry, M. P., Ochkur, S. I., Protheroe, C. A., Doyle, A., Grant, C. S., Cook-Mills, J., Birnbaumer, L., Lee, N. A., and Lee J. J. (2008) Allergic pulmonary inflammation promotes the recruitment of circulating tumor cells to the lung. *Cancer Res.* **68,** 8582–8589
2. Nakayama, T., Yao, L., and Tosato, G. (2004) Mast cell-derived angiopoietin-1 plays a critical role in the growth of plasma cell tumors. *J. Clin. Invest.* **114,** 1317–1325
3. Mizuno, H., Nakayama, T., Miyata, Y., Saito, S., Nishiwaki, S., Nakao, N., Takeshita, K., and Naoe, T. (2012) Mast cells promote the growth of Hodgkin's lymphoma cell tumor by modifying the tumor microenvironment that can be perturbed by bortezomib. *Leukemia* **26,** 2269–2276
4. de Souza, D. A., Jr., Toso, V. D., Campos, M. R., Lara, V. S., Oliver, C., and Jamur, M. C. (2012) Expression of mast cell proteases correlates with mast cell maturation and angiogenesis during tumor progression. *PLoS One* **7,** e40790
5. Rabenhorst, A., Schlaak, M., Heukamp, L. C., Förster, A., Theurich, S., von Bergwelt-Baildon, M., Büttner, R., Kurschat, P., Mauch, C., Roers, A., and Hartmann, K. (2012) Mast cells play a protumorigenic role in primary cutaneous lymphoma. *Blood* **120,** 2042–2054
6. Soucek, L., Lawlor, E. R., Soto, D., Shchors, K., Swigart, L. B., and Evan, G. I. (2007) Mast cells are required for angiogenesis and macroscopic expansion of Myc-induced pancreatic islet tumors. *Nat. Med.* **13,** 1211–1218
7. Jeong, H. J., Oh, H. A., Nam, S. Y., Han, N. R., Kim, Y. S., Kim, J. H., Lee, S. J., Kim, M. H., Moon, P. D., Kim, H. M., and Oh, H. A. (2013) The critical role of mast cell-derived hypoxia-inducible factor-1α in human and mice melanoma growth. *Int. J. Cancer* **132,** 2492–2501
8. Raica, M., Cimpean, A. M., Ceausu, R., Ribatti, D., and Gaje, P. (2013) Interplay between mast cells and lymphatic vessels in different molecular types of breast cancer. *Anticancer Res.* **33,** 957–963
9. Chang, D. Z. (2012) Mast cells in pancreatic ductal adenocarcinoma. *Oncoimmunology* **15,** 754–755
10. Rudolph, M. I., Boza, Y., Yefi, R., Luza, S., Andrews, E., Penissi, A., Garrido, P., and Rojas, I. G. (2008) The influence of mast cell mediators on migration of sw756 cervical carcinoma cells. *J. Pharmacol. Sci.* **106,** 208–218
11. Coussens, L. M., Raymond, W. W., Bergers, G., Laig-Webster, M., Behrendtsen, O., Werb, Z., Caughey, G. H., and Hanahan, D. (1999) Inflammatory mast cells upregulate angiogenesis during squamous epithelial carcinogenesis. *Genes Dev.* **13,** 1382–1397
12. Huang, B., Lei, Z., Zhang, G. M., Li, D., Song, C., Li, B., Liu, Y., Yuan, Y., Unkeless, J., Xiong, H., and Feng, Z. H. (2008) SCF mediated mast cell infiltration and activation exacerbate the inflammation and immunosuppression in tumor microenvironment. *Blood* **112,** 1269–1279
13. Olivera, A., Dillahunt, S. E., and Rivera, J. (2013) Interrogation of sphingosine-1-phosphate receptor 2 function *in vivo* reveals a prominent role in the recovery from IgE- and IgG-mediated anaphylaxis with minimal effect on its onset. *Immunol. Lett.* **150,** 89–96
14. Khan, B. Q., and Kemp, S. F. (2011) Pathophysiology of anaphylaxis. *Curr. Opin. Allergy Clin. Immunol.* **11,** 319–325
15. Song, Y., Qu, C., Srivastava, K., Yang, N., Busse, P., Zhao, W., and Li, X. M. (2010) Food allergy herbal formula 2 protection against peanut anaphylactic reaction is via inhibition of mast cells and basophils. *J. Allergy Clin. Immunol.* **126,** 1208–1217
16. Falanga, Y. T., Chaimowitz, N. S., Charles, N., Finkelman, F. D., Pullen, N. A., Barbour, S., Dholaria, K., Faber, T., Kolawole, M., Huang, B., Odom, S., Rivera, J., Carlyon, J., Conrad, D. H., Spiegel, S., Oskeritzian, C. A., and Ryan, J. J. (2012) Lyn but not Fyn kinase controls IgG-mediated systemic anaphylaxis. *J. Immunol.* **188,** 4360–4368
17. Bhavsar, P., Ahmad, T., and Adcock, I. M. (2008) The role of histone deacetylases in asthma and allergic diseases. *J. Allergy Clin. Immunol.* **121,** 580–584
18. Lu, T. X., Hartner, J., Lim, E. J., Fabry, V., Mingler, M. K., Cole, E. T., Orkin, S. H., Aronow, B. J., and Rothenberg, M. E. (2011) MicroRNA-21 limits *in vivo* immune response-mediated activation of the IL-12/IFN-γ pathway, Th1 polarization, and the severity of delayed-type hypersensitivity. *J. Immunol.* **187,** 3362–3373
19. Cao, D., Bromberg, P. A., and Samet, J. M. (2007) COX-2 expression induced by diesel particles involves chromatin modification and degradation of HDAC1. *Am. J. Respir. Cell Mol. Biol.* **37,** 232–239
20. Adcock, I. M., Ford, P., Ito, K., and Barnes, P. J. (2006) Epigenetics and airways disease. *Respir. Res.* **7,** 21
21. Choi, J. H., Oh, S. W., Kang, M. S., Kwon, H. J., Oh, G. T., and Kim, D. Y. (2005) Trichostatin A attenuates airway inflammation in mouse asthma model. *Clin. Exp. Allergy* **35,** 89–96
22. Zhu, H., Shan, L., Schiller, P. W., Mai, A., and Peng, T. (2010) Histone deacetylase-3 activation promotes tumor necrosis factor-α (TNF-α) expression in cardiomyocytes during lipopolysaccharide stimulation. *J. Biol. Chem.* **285,** 9429–9436
23. Kim, Y., Kim, K., Park, D., Lee, E., Lee, H., Lee, Y. S., Choe, J., and Jeoung, D. (2012) Histone deacetylase 3 mediates allergic skin inflammation by regulating expression of MCP1 protein. *J. Biol. Chem.* **287,** 25844–25859
24. Sharma, A., Kumar, M., Ahmad, T., Mabalirajan, U., Aich, J., Agrawal, A., and Ghosh, B. (2012) Antagonism of mmu-mir-106a attenuates asthma features in allergic murine model. *J. Appl. Physiol.* **113,** 459–464

[4] D. Jeoung, unpublished observations.

Downloaded from http://www.jbc.org/ at Università degli Studi di Roma on June 18, 2017

25. Song, C., Ma, H., Yao, C., Tao, X., and Gan, H. (2012) Alveolar macrophage-derived vascular endothelial growth factor contributes to allergic airway inflammation in a mouse asthma model. *Scand. J. Immunol.* **75,** 599–605
26. Panganiban, R. P., Pinkerton, M. H., Maru, S. Y., Jefferson, S. J., Roff, A. N., and Ishmael, F. T. (2012) Differential microRNA expression in asthma and the role of miR-1248 in regulation of IL-5. *Am. J. Clin. Exp. Immunol.* **1,** 154–165
27. Kumar, M., Ahmad, T., Sharma, A., Mabalirajan, U., Kulshreshtha, A., Agrawal, A., and Ghosh, B. (2011) Let-7 microRNA-mediated regulation of IL-13 and allergic airway inflammation. *J. Allergy Clin. Immunol.* **128,** 1077–1085
28. Polikepahad, S., Knight, J. M., Naghavi, A. O., Oplt, T., Creighton, C. J., Shaw, C., Benham, A. L., Kim, J., Soibam, B., Harris, R. A., Coarfa, C., Zariff, A., Milosavljevic, A., Batts, L. M., Kheradmand, F., Gunaratne, P. H., and Corry, D. B. (2010) Proinflammatory role for let-7 microRNAS in experimental asthma. *J. Biol. Chem.* **285,** 30139–30149
29. Collison, A., Mattes, J., Plank, M., and Foster, P. S. (2011) Inhibition of house dust mite-induced allergic airways disease by antagonism of microRNA-145 is comparable to glucocorticoid treatment. *J. Allergy Clin. Immunol.* **128,** 160–167
30. Kim, Y., Eom, S., Kim, K., Lee, Y. S., Choe, J., Hahn, J. H., Lee, H., Kim, Y. M., Ha, K. S., Ro, J. Y., and Jeoung, D. (2010) Transglutaminase II interacts with rac1, regulates production of reactive oxygen species, expression of snail, secretion of Th2 cytokines and mediates *in vitro* and *in vivo* allergic inflammation. *Mol. Immunol.* **47,** 1010–1022
31. Ujike, A., Ishikawa, Y., Ono, M., Yuasa, T., Yoshino, T., Fukumoto, M., Ravetch, J. V., and Takai, T. (1999) Modulation of immunoglobulin (Ig)E-mediated systemic anaphylaxis by low-affinity Fc receptors for IgG. *J. Exp. Med.* **189,** 1573–1579
32. Qi, D., Bergman, M., Aihara, H., Nibu, Y., and Mannervik, M. (2008) Drosophila Ebi mediates Snail-dependent transcriptional repression through HDAC3-induced histone deacetylation. *EMBO J.* **27,** 898–909
33. Kim, Y., Kim, K., Park, D., Lee, E., Lee, H., Lee, Y. S., Choe, J., Kim, Y. M., and Jeoung, D. (2013) DNA methyltransferase I acts as a negative regulator of allergic skin inflammation. *Mol. Immunol.* **53,** 1–14
34. Tominaga, T., Miyazaki, D., Sasaki, S., Mihara, S., Komatsu, N., Yakura, K., and Inoue, Y. (2009) Blocking mast cell-mediated type I hypersensitivity in experimental allergic conjunctivitis by monocyte chemoattractant protein-1/CCR2. *Invest. Ophthalmol. Vis. Sci.* **50,** 5181–5188
35. Na, Y. R., Yoon, Y. N., Son, D. I., and Seok, S. H. (2013) Cyclooxygenase-2 inhibition blocks M2 macrophage differentiation and suppresses metastasis in murine breast cancer model. *PLoS One* **8,** e63451
36. Hayashi, A., Horiuchi, A., Kikuchi, N., Hayashi, T., Fuseya, C., Suzuki, A., Konishi, I., and Shiozawa, T. (2010) Type-specific roles of histone deacetylase (HDAC) overexpression in ovarian carcinoma: HDAC1 enhances cell proliferation and HDAC3 stimulates cell migration with downregulation of E-cadherin. *Int. J. Cancer* **127,** 1332–1346
37. Wu, M. Z., Tsai, Y. P., Yang, M. H., Huang, C. H., Chang, S. Y., Chang, C. C., Teng, S. C., and Wu, K. J. (2011) Interplay between HDAC3 and WDR5 is essential for hypoxia-induced epithelial-mesenchymal transition. *Mol. Cell* **43,** 811–822
38. Huerta-Yepez, S., Baay-Guzman, G. J., Bebenek, I. G., Hernandez-Pando, R., Vega, M. I., Chi, L., Riedl, M., Diaz-Sanchez, D., Kleerup, E., Tashkin, D. P., Gonzalez, F. J., Bonavida, B., Zeidler, M., and Hankinson, O. (2011) Hypoxia-inducible factor promotes murine allergic airway inflammation and is increased in asthma and rhinitis. *Allergy* **66,** 909–918
39. Loubaki, L., Semlali, A., Boisvert, M., Jacques, E., Plante, S., Aoudjit, F., Mourad, W., and Chakir, J. (2010) Crosstalk between T cells and bronchial fibroblasts obtained from asthmatic subjects involves CD40L/α5 β1 interaction. *Mol. Immunol.* **47,** 2112–2118
40. Meyts, I., Hellings, P. W., Hens, G., Vanaudenaerde, B. M., Verbinnen, B., Heremans, H., Matthys, P., Bullens, D. M., Overbergh, L., Mathieu, C., De Boeck, K., and Ceuppens, J. L. (2006) IL-12 contributes to allergen-induced airway inflammation in experimental asthma. *J. Immunol.* **177,** 6460–6470
41. Chen, Q., and Massagué, J. (2012) Molecular pathways: VCAM-1 as a potential therapeutic target in metastasis. *Clin. Cancer Res.* **18,** 5520–5525
42. Leifheit-Nestler, M., Conrad, G., Heida, N. M., Limbourg, A., Limbourg, F. P., Seidler, T., Schroeter, M. R., Hasenfuss, G., Konstantinides, S., and Schäfer, K. (2010) Overexpression of integrin β5 enhances the paracrine properties of circulating angiogenic cells via Src kinase-mediated activation of STAT3. *Arterioscler. Thromb. Vasc. Biol.* **30,** 1398–1406
43. Matoba, K., Kawanami, D., Ishizawa, S., Kanazawa, Y., Yokota, T., and Utsunomiya, K. (2010) Rho-kinase mediates TNF-α-induced MCP-1 expression via p38 MAPK signaling pathway in mesangial cells. *Biochem. Biophys. Res. Commun.* **402,** 725–730
44. Lee, S. H., Kang, H. Y., Kim, K. S., Nam, B. Y., Paeng, J., Kim, S., Li, J. J., Park, J. T., Kim, D. K., Han, S. H., Yoo, T. H., and Kang, S. W. (2012) The monocyte chemoattractant protein-1 (MCP-1)/CCR2 system is involved in peritoneal dialysis-related epithelial-mesenchymal transition of peritoneal mesothelial cells. *Lab. Invest.* **92,** 1698–1711
45. Pande, K., Ueda, R., Machemer, T., Sathe, M., Tsai, V., Brin, E., Delano, M. J., Van Rooijen, N., McClanahan, T. K., Talmadge, J. E., Moldawer, L. L., Phillips, J. H., and LaFace, D. M. (2009) Cancer-induced expansion and activation of $CD11b^+$ $Gr\text{-}1^+$ cells predispose mice to adenoviral-triggered anaphylactoid-type reactions. *Mol. Ther.* **17,** 508–515
46. Mayoral, R. J., Deho, L., Rusca, N., Bartonicek, N., Saini, H. K., Enright, A. J., and Monticelli, S. (2011) MiR-221 influences effector functions and actin cytoskeleton in mast cells. *PLoS One* **6,** e26133
47. Mayoral, R. J., and Monticelli, S. (2010) Stable overexpression of miRNAs in bone marrow-derived murine mast cells using lentiviral expression vectors. *Methods Mol. Biol.* **667,** 205–214

Downloaded from http://www.jbc.org/ at Università degli Studi di Roma on June 18, 2017

Histone Deacetylase-3 Mediates Positive Feedback Relationship between Anaphylaxis and Tumor Metastasis

Sangkyung Eom, Youngmi Kim, Deokbum Park, Hansoo Lee, Yun Sil Lee, Jongseon Choe, Young Myeong Kim and Dooil Jeoung

J. Biol. Chem. 2014, 289:12126-12144.
doi: 10.1074/jbc.M113.521245 originally published online March 11, 2014

Access the most updated version of this article at doi: 10.1074/jbc.M113.521245

Alerts:
- When this article is cited
- When a correction for this article is posted

Click here to choose from all of JBC's e-mail alerts

This article cites 47 references, 17 of which can be accessed free at
http://www.jbc.org/content/289/17/12126.full.html#ref-list-1

Downloaded from http://www.jbc.org/ at Università degli Studi di Roma on June 18, 2017